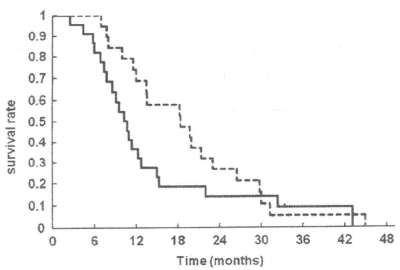

Fig. 1 Kaplan–Meier survival curves for recurrent MG cases treated by BNCT. The continuous line shows the survival of all patients after BNCT ($n = 22$). The broken line shows the survival of GBM (on-study histology) after diagnosis of GBM ($n = 19$)

Results

Survival after BNCT and after diagnosis

Individual histology (initial and on-study at relapse), RPA class, TMZ use, BNCT protocol (1 or 2), absorbed dose by BNCT, survival period after BNCT, and cause of death are summarized in Table 2. Survival after BNCT ($n = 22$) and that from initial GBM diagnosis ($n = 19$, on-study histology as GBM) are shown in Fig. 1. MST after BNCT for all patients ($n = 22$) was 10.8 months (95% CI, 7.3–12.8 months). MST after BNCT for GBM cases as on-study histology at recurrence ($n = 19$) was 9.6 months (95% CI, 6.9–11.4 months). MST after initial GBM diagnosis ($n = 19$) was 19.1 months (95% CI, 11.6–23.0 months).

Survival with special reference to RPA classes

The MSTs (months) of our BNCT cases classified according to RPA classes are shown in Table 3 and compared in each case with the values from Carson et al.: Class 1 ($n = 2$): 32.6 vs. 25.7 (Carson et al.), Class 2 ($n = 4$): 23.7 vs. 17.2, Class 3 ($n = 5$): 9.1 vs. 3.8, Class 4 ($n = 3$): 10.2 vs. 10.4, Class 5 ($n = 2$): 8.5 vs. 6.4, Class 7 ($n = 6$): 9.8 vs. 4.9. The tendencies in patient survival of our cases after BNCT were very similar to those of the original report in terms of RPA classification. Since our cases were so limited in number, we joined the worst prognosis classes (Class 3 and 7) together into one class. The MST of our cases in this combined class was 9.1 months ($n = 11$; 95% CI, 4.4–11.0 months), while that in Carson et al. was 4.4 months ($n = 129$; 95% CI, 3.6–5.4 months).

Cause of death after BNCT

We lost 21 cases out of 22. The causes of deaths were CSF dissemination (10 cases), local TP (5), both (1), RN (3), and other (2), as shown in Table 2. With regard to RN, we discuss more extensively in "Discussion".

Adverse effects of BNCT

No serious adverse effects were observed both in protocols 1 and 2 in this study of BNCT for recurrent MGs, even though all patients were applied with radiotherapy previously. Hematuria was reported in the literature using large amounts of BPA in BNCT [14]. Fortunately, we did not experience this adverse effect at all, however, three cases in protocol 2 showed transient decrease volume and turbidity of urine and fever during the first 24 h after BNCT. We concluded these side effects were caused by recrystallization of BPA in urine. Thereafter, we over hydrated the remaining patients after BNCT, and no such side effects were observed again.

Univariate analysis for the survival after BNCT

In Table 4, we analyzed factors for survival after BNCT, such as sex, age, TMZ or steroid usage, KPS, minimum absorbed dose in tumors, initial histology, GTV at the relapse, BNCT protocol (1 or 2) and RPA classes. Among them, only RPA class (RPA class 3 and 7 or others) showed a statistical significant influence on survival after BNCT.

Table 3 Comparison of NABTT trials and our BNCT series

	All patients			RPA 3 + 7		
	MST	95% CI	Number in series	MST	95% CI	Number in series
NABTT	7.0	6.2–8.0	$n = 310$	4.4	3.6–5.4	$n = 129$
BNCT	10.8	7.3–12.8	$n = 22$	9.1	4.4–11.0	$n = 11$

[a] New Approaches to brain tumor therapy CNS Consortium; 10 phase-1 and -2 trials reported by Carson et al. (J Clin Oncol 25:2601–2606, 2007)

MST, Median survival time; CI, confidence interval

Table 4 Univariate analysis of factors for survival after BNCT

Factor	Group	Survival (months)				*P*-Value
		Median	95% CI			
Sex	Male ($n = 15$)	9.1	6.0	–	11.0	$P = 0.2456$
	Female ($n = 7$)	12.8	5.8	–	22.0	
Age	≦50 ($n = 11$)	11.4	6.0	–	15.3	$P = 0.2482$
	>50 ($n = 11$)	9.1	5.8	–	12.3	
	≦57 ($n = 16$)	11.4	7.4	–	15.3	$P = 0.0982$
	>57 ($n = 6$)	10.8	2.5	–		
KPS	≦80 ($n = 13$)	9.6	6.0	–	11.4	$P = 0.1271$
	>80($n = 9$)	12.8	5.8	–		
Initial Histology	GBM ($n = 11$)	10.3	6.0	–	12.3	$P = 0.1329$
	Not GBM ($n = 11$)	10.8	4.4	–	32.4	
TMZ	Used ($n = 10$)	12.3	5.8	–	22.0	$P = 0.1468$
	Not used ($n = 12$)	9.6	4.4	–	15.0	
Steroid	Used ($n = 13$)	9.6	6.9	–	11.4	$P = 0.1445$
	Not used ($n = 9$)	12.8	2.5	–		
GTV (ml)	≦37.2($n = 11$)	9.1	4.4	–	12.8	$P = 0.5273$
	>37.2 ($n = 11$)	10.8	7.4	–	15.3	
Minimum tumor	≦34.0($n = 12$)	9.6	2.5	–	15.3	$P = 0.9110$
Dose (Gy-Eq)	>34.0($n = 10$)	11.0	6.0	–	12.8	
	≦37.0($n = 13$)	9.6	5.8	–	15.0	$P = 0.6548$
	>37.0($n = 9$)	11.4	6.0	–	22.0	
BNCT protocol	1 ($n = 9$)	9.6	2.5	–	15.3	$P = 0.8184$
	2 ($n = 13$)	11.0	6.9	–	12.8	
RPA class	RPA 3&7 ($n = 11$)	9.1	4.4	–	11.0	$P = 0.0216$
	RPA not 3&7 ($n = 11$)	12.8	6.9	–	32.4	

Representative case

A 48-year-old man with a right temporal mass was operated emergently for consciousness disturbance in a hospital. The operation was partial tumor removal and histological diagnosis was GBM. He received fractionated X-ray radiation therapy (XRT) with a total dose of 80 Gy and chemotherapy consisting of nimustine and vincristine. Even during the radiotherapy, the tumor continued to enlarge, and the patient was referred to our institute for BNCT (Fig. 2 a, a′). He was classified as RPA class 4. The BNCT was performed with the minimum tumor absorbed dose of 27.2 Gy-Eq, and maximum brain absorbed dose of 11.1 Gy-Eq. One week after BNCT the mass shrunk rapidly (Fig. 2 b, b′). Three months after BNCT, the original mass became enlarged in Gd-MRI. He was operated on again. The histology was mainly necrosis with small pocket of residual tumor cells. He was well for another 4 months. We lost this case 7.8 months after BNCT and 13.5 months after initial surgery, due to CSF dissemination (Fig. 2 c, c′). This is a representative case of recurrent MG treated by BNCT, with regard to the rapid tumor shrinkage after BNCT and the occurrence of radiation necrosis and CSF dissemination as the cause of death.

Discussion

Here we reported the survival benefit of BNCT for recurrent MG cases, mainly GBM. The MST after BNCT for GBM cases as on-study histology at recurrence ($n = 19$) was 9.6 months (95% CI, 6.9–11.4 months). In the literature, we found a summary of a large series of eight phase-2 trials of chemotherapies for recurrent GBM cases [15]. In this report, the authors mentioned the MST of GBM after relapse as 25 weeks (5.8 months; 95% CI, 21–28 weeks, 4.9–6.5 months; $n = 225$). In comparison with this result, our data for the survival benefit of BNCT in recurrent GBM was not bad.

As to BNCT for recurrent GBM, two small series have been reported in the literature. A Swedish group and a Finnish group reported that MSTs for recurrent GBM after BNCT were 8.7 ($n = 12$) [16] and 7.5 months ($n = 7$) [17], respectively. Our data in the current report is almost equal to/somewhat better than the findings in these reports.

Kaplan–Meyer analysis in Fig. 1 showed that MST after BNCT for all patients ($n = 22$) was 10.8 months (95% CI, 7.3–12.8 months). We are not sure whether this result is reliable, as this is the result of a small series from a single institute. To evaluate the survival benefit of BNCT in low

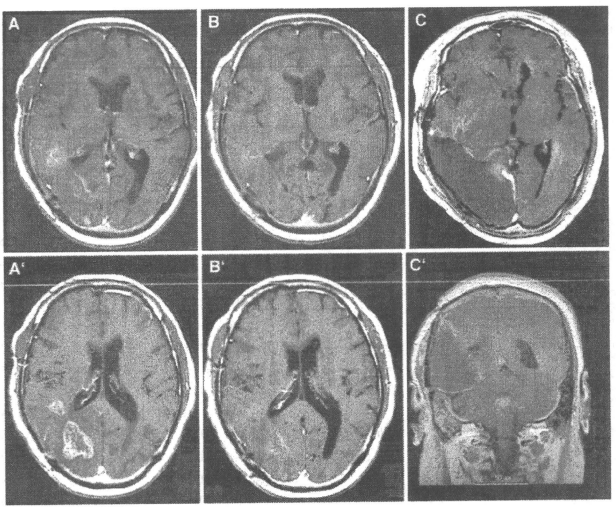

Fig. 2 A representative case of recurrent GBM treated by BNCT. (**a**, **a'**) MRI, prior to BNCT. Gd-enhanced lesions were at the right temporo-occipital lobe; (**b**, **b'**) MRI, 48 h after BNCT. Marked shrinkage of the lesions was recognized; (**c**, **c'**) MRI, 7 months after BNCT. CSF dissemination was prominent

and high-risk group of recurrent MGs, we applied RPA to our cases as advocated in the literature [8]. Inclusion criteria for our trial and the 10 NABTT phase-1 and -2 trials reported in Carson et al. were not very different. Our case numbers for each RPA class were so limited, however, that the MST of our cases in each RPA class were relatively better in comparison with original NABTT results, as listed above. In the original article, RPA class 3 (Not GBM, KPS $\leq$ 70) and class 7 (GBM, Age $\geq$ 50, steroid use) showed extremely poor prognosis (supplementary Table 1). The MST of our combined class 3 and class 7 cases was 9.1 months ($n = 11$; 95% CI, 4.4–11.0 months), while that in the original article was 4.4 months ($n = 129$; 95% CI, 3.6–5.4 months). We cannot know whether our current MST data is significantly better than that of each NABTT trial because their raw data were not available. But at least, BNCT showed a good survival benefit even for the highest-risk group, RPA class 3 and 7.

TMZ is the sole promising drug for GBM so far. A Swedish BNCT group reported potential TMZ effects with combination of BNCT at the relapse of GBM [16]. However, in our univariate analysis, TMZ did not contribute prominently to the prolongation of survival in our series (Table 4). In our 22 cases, we used TMZ in 10 cases, before BNCT in 3 cases (Cases 11, 14 and 16) and after BNCT in 7 (Cases 1, 2, 3, 13, 20, 21 and 22). For the former three cases, TMZ could not control the tumor growth and methylation-specific PCR showed an unmethylated O6-methylguanine DNA methyltransferase (MGMT) promoter [18] (data not shown). We stopped the administration of TMZ after BNCT as we judged TMZ was not efficacious for these three cases. Among the latter seven cases, only two (Cases 1 and 2, both classified as RPA class 1) showed methylated promoter status for MGMT, with good prognoses. For the other five cases, we were not sure of the MGMT expression status of the tumor. In the high-risk group in our series (RPA class 3 and 7), three cases were administered TMZ after BNCT (Cases 20, 21 and 22). Among them, Case 21 and 22 showed a relatively short survival after BNCT. We do not deny the meaning of TMZ use at relapse; however, in our series for this high-risk group, the survival benefit of TMZ was limited. In the literature, TMZ has actually shown modest survival benefit at relapse of recurrent GBM [19]. Brada et al. reported only 5.4 months prolongation as MST with TMZ at relapse in the report.

There are several reports with relatively good results for recurrent MG, with an MST of around 10 months after the stereotactic radiosurgery (SRS) [20] or stereotactic radiotherapy (SRT) [21] at relapse. However, there was big difference in GTV at the relapse between these SRS or SRT cases and ours. The median GTV of the former two was 10.1 and 12.7 ml, while the median GTV of our cases was 42.0 ml. There might also be a difference as to performance status or age between the SRS or SRT reports and our cases. The result of re-irradiation for recurrent

GBM was poor [22]. The MST of this report was 26 weeks after the treatment. In addition, BNCT can be applied in only one day. Taken together, BNCT could be one of the promising radiation treatment options for recurrent MG at relapse.

We lost many cases of recurrent MGs after BNCT by CSF dissemination, as we reported (in preparation) and as shown in Table 2 and Fig. 2. In other words, local control by BNCT for even recurrent MG was fairly good. There was a tendency for CSF dissemination to occur in relatively long-term survivors from diagnosis (data not shown). On the other hand, a major problem in BNCT for recurrent MG was the occurrence of RN. We experienced RN by BNCT especially for recurrent MG, because the patients had been treated by radiotherapy prior to BNCT. Although BNCT is cell-selective particle radiation, some particle dose is inevitably absorbed by the normal brain tissue as shown in Table 2. The diagnosis of this pathology is difficult; however, amino acid PET may give us good clue for it, as stated above [12]. Most of RN could be controlled with medical or surgical treatments as above; however, we lost three cases by RN in our series. Preventive medical treatments such as by anticoagulants or by vitamin E must be considered after BNCT, especially for recurrent cases. This is not mentioned in other BNCT reports for recurrent MG [16, 17]; however, it should be seriously considered. In Swedish reports of BNCT for recurrent GBM, the authors mentioned a median time to tumor progression of 6 months after BNCT, but there was no statement as to how TP was judged in their report. It is very difficult to differentiate RN and TP on MRI, especially with high-dose radiation treatment. So we did not apply the analysis of time to tumor progression in our series. In univariate analysis (Table 4), there was no correlation of minimum tumor dose by BNCT and survival after BNCT. Especially for recurrent cases, if we increase the minimum tumor dose by BNCT, the incidence of RN probably increases, as discussed here. Therefore, it is very difficult to elucidate the most suitable dose of BNCT at relapse. Regardless, RN is a serious problem to be overcome in the field of BNCT.

XRT plus concomitant TMZ (Stupp's regimen) has been the global standard so far for newly diagnosed GBM [23]. Pellettieri et al. reported that BNCT at relapse after Stupp's regimen might be the best treatment of GBM [16]. Also in our series BNCT at relapse showed a good MST after the initial GBM diagnosis of 19.1 months ($n = 19$; 95% CI, 11.6–23.0 months). But it cannot be concluded so easily that BNCT at relapse after Stupp's regimen is the best for the treatment of GBM because 19 cases in our series were referred to our institute at relapse with a significant interval after initial treatments. This interval might prolong the survival after initial GBM diagnosis at a glance.

In summary, the RPA classification advocated by Carson et al. predicted the patient survival trends of our BNCT series; however, BNCT showed the most prominent survival benefit in the high-risk group (RPA classes 3 and 7).

Acknowledgments This work was partly supported by Grants-in-Aid for Scientific Research (B) (16390422 and 19390385) from the Japanese Ministry of Education, Science and Culture, by a Grant-in-Aid for Scientific Research from the Ministry of Health, Labor and Welfare of Japan to S–I.M. (P·I., Hideki Matsui) and by the Regional Science Promotion Program of the Japan Science and Technology Corporation, as well as by the "Second-term Comprehensive 10-Year Strategy for Cancer Control" of the Ministry of Health, Labor, and Welfare of Japan to S–I.M. This work was also supported in part by the Takeda Science Foundation for Osaka Medical College, by a Grant-in-Aid for Cancer Research from the Ministry of Education, Culture, Sports, Science, and Technology of Japan (12217065) to K. O., and by Grants-in-Aid for Scientific Research by young researchers (B) (18791030) from the Japanese Ministry of Education, Science, and Culture to S. K. The top two authors contributed equally in this study as primary co-investigators.

References

1. Kawabata S, Miyatake S, Kajimoto Y et al (2003) The early successful treatment of glioblastoma patients with modified boron neutron capture therapy: report of two cases. J Neurooncol 65:159–165. doi:10.1023/B:NEON.0000003751.67562.8e
2. Miyatake S, Kawabata S, Kajimoto Y et al (2005) Modified boron neutron capture therapy for malignant gliomas performed using epithermal neutron and two boron compounds with different accumulation mechanisms: an efficacy study based on findings on neuroimages. J Neurosurg 103:1000–1009
3. Miyatake S, Tamura Y, Kawabata S et al (2007) Boron neutron capture therapy for malignant tumors related to meningiomas. Neurosurgery 61:82–90. doi:10.1227/01.neu.0000279727.90650.24 Discussion 90–81
4. Tamura Y, Miyatake S, Nonoguchi N et al (2006) Boron neutron capture therapy for recurrent malignant meningioma: case report. J Neurosurg 105:898–903. doi:10.3171/jns.2006.105.6.898
5. Coderre JA, Chanana AD, Joel DD et al (1998) Biodistribution of boronophenylalanine in patients with glioblastoma multiforme: boron concentration correlates with tumor cellularity. Radiat Res 149:163–170. doi:10.2307/3579926
6. Huncharek M, Muscat J (1998) Treatment of recurrent high grade astrocytoma; results of a systematic review of 1, 415 patients. Anticancer Res 18:1303–1311
7. Kawabata S, Miyatake S, Kuroiwa T et al Boron neutron capture therapy for newly diagnosed glioblastoma. J Rad Res (in press)
8. Carson KA, Grossman SA, Fisher JD et al (2007) Prognostic factors for survival in adult patients with recurrent glioma enrolled onto the new approaches to brain tumor therapy CNS consortium phase I and II clinical trials. J Clin Oncol 25:2601–2606. doi:10.1200/JCO.2006.08.1661
9. Imahori Y, Ueda S, Ohmori Y et al (1998) Positron emission tomography-based boron neutron capture therapy using boronophenylalanine for high-grade gliomas: part II. Clin Cancer Res 4:1833–1841
10. Imahori Y, Ueda S, Ohmori Y et al (1998) Positron emission tomography-based boron neutron capture therapy using boronophenylalanine for high-grade gliomas: part I. Clin Cancer Res 4:1825–1832

11. Sakurai Y, Ono K, Miyatake S et al (2006) Improvement effect on the depth-dose distribution by CSF drainage and air infusion of a tumour-removed cavity in boron neutron capture therapy for malignant brain tumours. Phys Med Biol 51:1173–1183. doi:10.1088/0031-9155/51/5/009
12. Miyashita M, Miyatake S, Imahori Y et al (2008) Evaluation of fluoride-labeled boronophenylalanine-PET imaging for the study of radiation effects in patients with glioblastomas. J Neurooncol 89:239–246. doi:10.1007/s11060-008-9621-6
13. Glantz MJ, Burger PC, Friedman AH et al (1994) Treatment of radiation-induced nervous system injury with heparin and warfarin. Neurology 44:2020–2027
14. Henriksson R, Capala J, Michanek A et al (2008) Boron neutron capture therapy (BNCT) for glioblastoma multiforme: a phase II study evaluating a prolonged high-dose of boronophenylalanine (BPA). Radiother Oncol 88:183–191
15. Wong ET, Hess KR, Gleason MJ et al (1999) Outcomes and prognostic factors in recurrent glioma patients enrolled onto phase II clinical trials. J Clin Oncol 17:2572–2578
16. Pellettieri L, H-Stenstam B, Rezaei A et al (2008) An investigation of boron neutron capture therapy for recurrent glioblastoma multiforme. Acta Neurol Scand 117:191–197. doi:10.1111/j.1600-0404.2007.00924.x
17. Joensuu H, Kankaanranta L, Seppala T et al (2003) Boron neutron capture therapy of brain tumors: clinical trials at the Finnish facility using boronophenylalanine. J Neurooncol 62:123–134
18. Hegi ME, Diserens AC, Gorlia T et al (2005) MGMT gene silencing and benefit from temozolomide in glioblastoma. N Engl J Med 352:997–1003. doi:10.1056/NEJMoa043331
19. Brada M, Hoang-Xuan K, Rampling R et al (2001) Multicenter phase II trial of temozolomide in patients with glioblastoma multiforme at first relapse. Ann Oncol 12:259–266. doi:10.1023/A:1008382516636
20. Shrieve DC, Alexander E III, Wen PY et al (1995) Comparison of stereotactic radiosurgery and brachytherapy in the treatment of recurrent glioblastoma multiforme. Neurosurgery 36:275–282. doi:10.1097/00006123-199502000-00006 Discussion 282–274
21. Hudes RS, Corn BW, Werner-Wasik M et al (1999) A phase I dose escalation study of hypofractionated stereotactic radiotherapy as salvage therapy for persistent or recurrent malignant glioma. Int J Radiat Oncol Biol Phys 43:293–298. doi:10.1016/S0360-3016(98)00416-7
22. Veninga T, Langendijk HA, Slotman BJ et al (2001) Reirradiation of primary brain tumours: survival, clinical response and prognostic factors. Radiother Oncol 59:127–137. doi:10.1016/S0167-8140(01)00299-7
23. Stupp R, Mason WP, van den Bent MJ et al (2005) Radiotherapy plus concomitant and adjuvant temozolomide for glioblastoma. N Engl J Med 352:987–996. doi:10.1056/NEJMoa043330

Comparison of Postoperative Morphological Changes in Remnant Pancreas Between Pancreaticojejunostomy and Pancreaticogastrostomy After Pancreaticoduodenectomy

Yoshito Tomimaru, MD, Yutaka Takeda, MD,* Shogo Kobayashi, MD,* Shigeru Marubashi, MD,* Chun Man Lee, MD,* Masahiro Tanemura, MD,* Hiroaki Nagano, MD,* Toru Kitagawa, MD,* Keizo Dono, MD,* Koji Umeshita, MD,* Kenichi Wakasa, MD,† and Morito Monden, MD**

Objectives: The aim of this study was to compare postoperative morphological changes in remnant pancreas between pancreaticojejunostomy (PJ) and pancreaticogastrostomy (PG) after pancreaticoduodenectomy (PD).

Methods: The study subjects were 28 patients with PJ and 14 with PG. The diameter of the main pancreatic duct (MPD) and pancreatic parenchymal thickness 2 years after PD were measured on computed tomography scans and compared between the 2 groups.

Results: The preoperative and postoperative MPD diameter was 5.2 mm (SD, 2.4 mm) and 4.2 mm (SD, 2.0 mm) in the PJ group ($P = 0.0422$) and 4.8 mm (SD, 3.2 mm) and 5.7 mm (SD, 1.8 mm) ($P = 0.1494$) in the PG group, respectively. In those patients with preoperatively normal-size MPD, MPD after surgery tended to become dilated relative to before surgery in the PJ group ($P = 0.0931$), and the MPD measured postoperatively was significantly larger than preoperatively in the PG group ($P = 0.0009$). A significant atrophy of the pancreatic parenchyma was noted postoperatively in both groups ($P < 0.0001$), but these changes were more severe in the PG group than the PJ group ($P = 0.0018$).

Conclusions: Considering the above postoperative morphological changes, PJ seems to be preferable to PG after pancreaticoduodenectomy.

Key Words: pancreaticoduodenectomy, pancreaticogastrostomy, pancreaticojejunostomy, morphology, atrophy, duct dilatation

(*Pancreas* 2009;38: 203–207)

Pancreaticoduodenectomy (PD) is the standard procedure for neoplasms of periampullary lesions.[1] In this procedure, the cut end of the pancreas is usually anastomosed to either the jejunum (pancreaticojejunostomy [PJ]) or the stomach (pancreaticogastrostomy [PG]). Many previous authors have long compared these 2 types of anastomoses with regard to the incidence of pancreatic leakage, which is the leading cause of complication after PD in the early postoperative period.[2–5] With regard to the incidence of pancreatic leakage, some prospective randomized trials reported that there was no difference between PJ and PG.[6–8]

In addition to the incidence of pancreatic leakage, the exocrine and endocrine functions of the remnant pancreas have been compared. There is no significant difference between PJ and PG in terms of pancreatic endocrine function, whereas PG is associated with more severe or equal pancreatic exocrine insufficiency than PJ.[9–12] In these previous comparative studies, fasting blood glucose level, glycohemoglobin A_{1c}, oral glucose tolerance testing, and the status of diabetes mellitus were used for evaluation of pancreatic endocrine function, and the presence of steatorrhea, fecal elastase-1 test, and nutritional status were used for the evaluation of pancreatic exocrine function. When comparing the functions of the remnant pancreas, morphological evaluation of the remnant pancreas is necessary, in addition to the above parameters, because such function depends on the volume of pancreatic parenchymal tissue. However, there is limited information on the morphology of the remnant pancreas after PD.[13,14] In this study, we evaluated postoperative morphological changes in the remnant pancreas between PJ and PG after PD.

MATERIALS AND METHODS

Between 1999 and 2007, 156 patients who had benign and malignant neoplasms of periampullary lesions underwent PD without hepatic resection in the Department of Surgery, Osaka University Hospital. Among the 156 patients, 17 patients underwent PD including distal gastrectomy, 96 patients underwent subtotal stomach-preserving PD, and the remaining 43 patients underwent pylorus-preserving PD. To exclude the influence of differences in surgical procedures, only patients who underwent subtotal stomach-preserving PD and reconstruction by invagination method were included in this study.

The reconstruction procedure of PJ and PG was chosen based on surgeons' preference. In the PJ group, the pancreatic stump was anastomosed and invaginated end-to-end into the jejunum with interrupted 2-layer sutures: 4–0 absorbable monofilament for outer layer between the remnant pancreatic capsule and jejunal seromuscular layer and for inner layer between the cut edge of the pancreas and the full thickness of the jejunum. In the PG group, a gastrostomy of 2 to 3 cm in length was made in the posterior wall of the stomach, and the pancreatic stump was anastomosed and invaginated with the same interrupted 2-layer method as PJ. In both groups, a stenting tube was placed in the main pancreatic duct (MPD) and exteriorized through the abdominal wall via the wall of the jejunum or stomach. The tube was removed within 1 postoperative month.

In this study, the morphology of the remnant pancreas was evaluated 2 years after the surgery. Patients with intraductal papillary mucinous neoplasm of pancreas were excluded in this study because their preoperative MPD may be dilated for the disease itself. Thus, only patients who had survived 2 years or more without cancer recurrence were included in this study: 28 PJ patients (PJ group) and 14 patients (PG group).

The morphology of the remnant pancreas was examined using computed tomography.

From the *Department of Surgery, Graduate School of Medicine, Osaka University; and †Department of Pathology, Osaka City University Hospital, Osaka, Japan.

Received for publication April 21, 2008; accepted September 8, 2008.

Reprints: Yutaka Takeda, MD, Department of Surgery, Osaka University, Graduate School of Medicine, 2-2 Yamadaoka E-2, Suita City, Osaka 565-0871, Japan (e-mail: ytakeda@surg2.med.osaka-u.ac.jp).

TABLE 1. Comparison of Clinical Background Between the PJ and PG Groups

	PJ	PG	*P*
No. patients	28	14	
Age, mean (SD), yrs	64 [8]	62 [9]	0.3379
Sex (male/female)	13/15	5/9	0.5083
Origin of tumor			
Pancreas	23	11	
Bile duct	3	1	0.5439
Papilla Vater	2	1	
Duodenum	0	1	
Fibrosis (−/+)	9/19	5/9	>0.9999

The MPD diameter was measured manually in the region where the maximum MPD diameter was identified. The MPD was considered dilated if the diameter exceeded 3 mm.[11,13–15] The pancreatic parenchymal thickness was defined as the anterior-posterior width of the entire gland minus MPD diameter and was measured manually in the region of the pancreas where the maximum MPD diameter was identified. The following equations were used for our calculations:

Rate of reduction of MPD diameter = (preoperative MPD diameter − postoperative MPD diameter) / preoperative MPD diameter

Rate of reduction of pancreatic parenchymal thickness = (preoperative pancreatic parenchymal thickness − postoperative pancreatic parenchymal thickness) / preoperative pancreatic parenchymal thickness

Postoperatively, the degree of fibrosis in pancreatic parenchyma was microscopically examined by a pathologist who had no information on the clinical course of any patient. Then, patients included in this study were divided into 2 groups: fibrosis and no fibrosis.

Abdominal computed tomography scans were performed for postoperative follow-up at regular intervals of 3 to 6 months in patients with malignancy and 12 to 24 months in those with benign tumor.

Data were expressed as mean (SD). Differences between groups were examined for statistical significance using the χ^2, Fisher exact test, Mann-Whitney *U* test, or Wilcoxon signed rank test. $P < 0.05$ denoted the presence of a statistically significant difference. Statistical analyses were performed using StatView (version 5.0; SAS Institute Inc, Cary, NC). This study protocol was approved by the human ethics review committee of Osaka University Hospital, and a signed consent form was obtained from each patient.

RESULTS

Table 1 summarizes the clinical profile of patients of the PJ and PG groups. Patients of the 2 groups were similar with regard to age, sex, and origin of tumor. Most tumors in our cohort were malignant (PJ group: 28/28 [100%], PG group: 13/14 [93%]). The incidence of short-time postoperative complications including pancreatic leakage did not differ between the 2 groups. Fibrosis in pancreatic parenchymal was found in 19 cases (68%) in the PJ group and 9 cases (64%) in the PG group ($P > 0.9999$). Figure 1 shows the preoperative and postoperative values of MPD diameter, and Figure 2 depicts the respective values of pancreatic parenchymal thickness. Table 2 compares the morphological changes between the PJ and PG groups.

In more than half of the patients, the MPD was dilated before surgery (PJ group: 20/28 [71%], PG group: 9/14 [64%]). Among 8 patients of the PJ group who showed no preoperative MPD dilatation, 2 (25%) developed MPD dilatation after surgery. On the other hand, among 5 patients free of preoperative MPD dilatation in the PG group, all patients (100%) showed MPD dilatation after surgery.

The preoperative MPD diameter of the PJ group (5.2 mm [SD, 2.4 mm]) was not significantly different from that of the PG group (4.8 mm [SD, 3.2 mm], $P = 0.7079$). On the other hand, the postoperative MPD diameter of the PJ group (4.2 mm [SD, 2.2 mm]) was significantly smaller than that of the PG

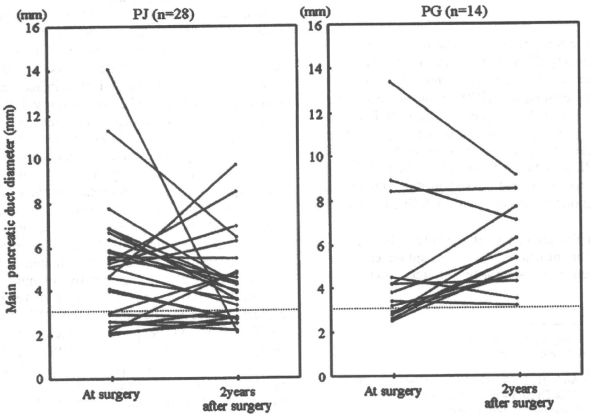

FIGURE 1. Individual data of diameter of the MPD at the time of surgery and 2 years after the surgery.

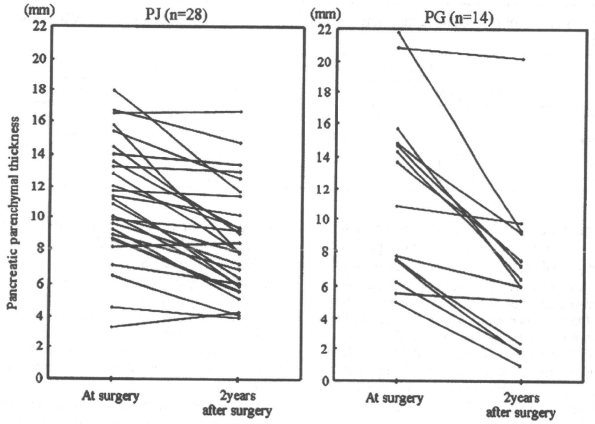

FIGURE 2. Individual data of pancreatic parenchymal thickness at the time of surgery and 2 years after the surgery.

group (5.7 mm [SD, 1.8 mm], $P = 0.0149$). In the PJ group, the MPD diameter after surgery was significantly smaller than that before surgery ($P = 0.0422$). On the other hand, the change in MPD diameter after surgery was not significant in the PG group ($P = 0.1494$). Finally, the rate of reduction of MPD diameter was significantly larger in the PJ (5.1% [SD, 48.3%]) than in the PG groups (−41.6% [SD, 53.9%], $P = 0.0070$).

The preoperative pancreatic parenchymal thickness was similar in the 2 groups (PJ: 11.1 mm [SD, 3.7 mm], PG: 11.8 mm [SD, 5.5 mm], $P = 0.58489$), and decreased significantly in both groups after surgery (PJ: $P < 0.0001$, PG: $P < 0.0001$), although the mean values were not different between the 2 groups (PJ: 8.4 mm [SD, 3.4 mm], PG: 6.7 mm [SD, 4.8 mm], $P = 0.1770$). However, the rate of reduction of pancreatic parenchymal thickness was significantly larger in the PG group (46.0% [SD, 25.9%]) than in the PJ group (22.4% [SD, 19.1%], $P = 0.0018$).

Next, we compared the MPD diameter in those patients of the PJ and PG groups who had a normal-size MPD preoperatively (PJ: n = 8, PG: n = 5) (Table 3). In these patients, the preoperative MPD diameter was similar (PJ: 2.5 mm [SD, 0.4], PG: 2.7 mm [SD, 0.2 mm], $P = 0.3421$). Postoperatively, the MPD diameter increased in the PJ group (3.1 mm [SD, 1.1 mm]), although insignificantly ($P = 0.0931$), whereas it became significantly larger in the PG group (5.3 mm [SD, 0.6 mm], $P = 0.0009$). In addition, the postoperative MPD diameter in the PJ group was significantly smaller than that in the PG group ($P = 0.0015$). The rate of reduction of MPD diameter was significantly larger in the PJ (−27.7% mm [SD, 45.0%]) than in the PG groups (−96.0% mm [SD, 24.4%], $P = 0.0070$).

Only in patients who had survived 3 years or more without cancer recurrence, the postoperative temporal changes in MPD diameter and pancreatic parenchymal thickness were compared (PJ: n = 8, PG: n = 7) (Fig. 3). In both groups, the postoperative changes of MPD diameter and pancreatic parenchymal thickness started just after the surgery and almost finished by 1 year after the operation.

DISCUSSION

The results of the present study showed that the postoperative MPD diameter was significantly smaller than the preoperative MPD only in the PJ group. However, because MPD was dilated preoperatively in more than half of patients enrolled in this study, we also examined the change in MPD diameter in those patients without preoperative MPD dilatation. Such

TABLE 2. Comparison of Morphological Changes Between the PJ and PG Groups

	PJ (n = 28)		PG (n = 14)		
	Mean (SD)	*P*	Mean (SD)	*P*	*P*
Diameter of the MPD, mean (SD)					
Before surgery, mm	5.2 [2.4]	0.0422	4.8 [3.2]	0.1494	0.7097
After surgery, mm	4.2 [2.0]		5.7 [1.8]		0.0149
Reduction rate, %	5.1 [48.3]		−41.6 [53.9]		0.0070
Parenchymal thickness, mean (SD)					
Before surgery, mm	11.1 [3.7]	<0.0001	11.8 [5.5]	<0.0001	0.5849
After surgery, mm	8.4 [3.4]		6.7 [4.8]		0.1770
Reduction rate, %	22.4 [19.1]		46.0 [25.9]		0.0018

TABLE 3. Comparison of Morphological Changes Between the PJ and PG Groups in a Subgroup With Nondilated MPD Preoperatively

	PJ (n = 8)		PG (n = 5)		
	Mean (SD)	*P*	Mean (SD)	*P*	*P*
Diameter of the MPD					
Before surgery, mm	2.5 [0.4]	0.0931	2.7 [0.2]	0.0009	0.3421
After surgery, mm	3.1 [1.1]		5.3 [0.6]		0.0015
Reduction rate, %	−27.7 [45.0]		−96.0 [24.4]		0.0106

analysis found that the MPD diameter after surgery tended to be larger than before surgery in the PJ group, and significantly larger in the PG group. To date, few studies have measured MPD diameter after PD, and their results suggested no significant difference in the rate of change of MPD diameter between the PJ and PG groups.[9,12] On the other hand, Sato et al[13] reported that among 19 patients with PJ, 8 (42%) demonstrated a decline in MPD diameter, 9 (47%) showed no change, and 2 (11%) developed MPD dilatation. Furthermore, Lemaire et al[14] reported that postoperative MPD was significantly dilated in patients with PG. The results of these previous studies are not necessarily compatible. The different results were probably due to patient selection, that is, the enrollment of patients with preoperative MPD dilatation. In fact, the proportion of patients with dilated MPD preoperatively has not been reported, and the change in MPD diameter has been examined only in patients with nondilated MPD preoperatively.[12–15] Thus, had the patients with preoperative MPD dilatation been excluded in the above studies, the results of the present study could have been similar.

The present study also showed that significant atrophy of the pancreatic parenchyma occurred after surgery in both groups. Few studies have examined this issue previously, although there has been no comparative study of pancreatic parenchymal atrophy between PJ and PG. Sato et al[13] reported that parenchymal atrophy of the remnant pancreas occurred in 9 (56%) of 16 patients with PJ. Lemaire et al[14] reported that pancreatic atrophy assessed by subtracting the MPD diameter from the total parenchymal thickness tended to develop in patients with PG, although the study was not comparative. Our results are consistent with those of the above studies. In addition, our study showed that the parenchymal atrophic changes in the PG group were significantly more severe than those in the PJ group.

The current study also revealed the temporal change in MPD diameter and pancreatic parenchymal thickness. To date, there have also been no studies of this issue.

The postoperative MPD dilatation and parenchymal atrophy are thought to result from obstruction or stenosis of the anastomosis.[13,14] However, to date, there have been few reports on pancreatic duct patency after PG. For example, Telford et al[16] showed that total obstruction of the pancreatic duct after PG occurred in 90% of animals in which the duct had been implanted into the stomach. On the other hand, Amano et al[17] reported that in 1 patient among 5 with PG who were followed up postoperatively for more than 9 years, the anastomotic site was not detected by gastroscopy because of overhealing by

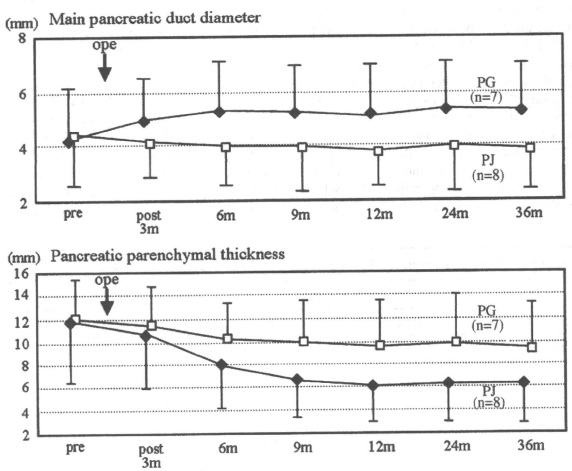

FIGURE 3. The temporal change in the diameter of the MPD and pancreatic parenchymal thickness during 3 postoperative years.

gastric mucosa. Unfortunately, the anastomotic patency was not examined in our study. However, taking into consideration that the anastomosis was performed by the invagination method in all patients, the patency may depend on different environment of the anastomosed remnant pancreas in both groups. The postoperative MPD dilatation and parenchymal atrophy, which was predominant in the PG group relative to the PJ group, could be due to the reflux of gastric juice or ingested food into the remnant pancreatic duct or coverage of the anastomotic orifice by gastric mucosa, which might induce chronic inflammation, stenosis, or obstruction of the anastomotic site.

Postoperative pancreatic function was not examined in this study. Previous studies indicated no significant differences in early postoperative complications and pancreatic endocrine function between PJ and PG, although patients who underwent PG showed more severe or equal pancreatic exocrine insufficiency than that of those who underwent PJ.[3–12] The difference in exocrine function may be natural, considering the postoperative morphological changes in this study.

In summary, only in PJ patients with preoperatively normal-size MPD the MPD after surgery tended to become dilated after surgery, whereas the MPD was significantly larger after surgery than before surgery in the PG group. Furthermore, significant atrophic changes were noted postoperatively in the pancreatic parenchyma in both groups, and these changes were significantly more severe in the PG group than the PJ group. Considering these postoperative morphological changes in the remnant pancreas, PJ may be preferable to PG after PD.

REFERENCES

1. Whipple AO, Parsons WB, Mullins CR. Treatment of carcinoma of the ampulla of Vater. *Ann Surg*. 1935;102:763–779.
2. Delcore R, Thomas JH, Pierce GE, et al. Pancreatogastrostomy: a safe drainage procedure after pancreatoduodenectomy. *Surgery*. 1990;108: 641–645.
3. Kim SW, Youk EG, Park YH. Comparison of pancreatogastrostomy and pancreatojejunostomy after pancreatoduodenectomy performed by one surgeon. *World J Surg*. 1997;21:640–643.
4. Kapur BM, Misra MC, Seenu V, et al. Pancreaticogastrostomy for reconstruction of pancreatic stump after pancreaticoduodenectomy for ampullary carcinoma. *Am J Surg*. 1998;176:274–278.
5. Arnaud JP, Tuech JJ, Cervi C, et al. Pancreaticogastrostomy compared with pancreaticojejunostomy after pancreaticoduodenectomy. *Eur J Surg*. 1999;165:357–362.
6. Yeo CJ, Cameron JL, Maher MM, et al. A prospective randomized trial of pancreaticogastrostomy versus pancreaticojejunostomy after pancreaticoduodenectomy. *Ann Surg*. 1995;222:580–588.
7. Bassi C, Falconi M, Molinari E, et al. Reconstruction by pancreaticojejunostomy versus pancreaticogastrostomy following pancreatectomy: results of a comparative study. *Ann Surg*. 2005;242: 767–771.
8. Duffas JP, Suc B, Msika S, et al. A controlled randomized multicenter trial of pancreatogastrostomy or pancreatojejunostomy after pancreatoduodenectomy. *Am J Surg*. 2005;189:720–729.
9. Konishi M, Ryu M, Kinoshita T, et al. Pathophysiology after pylorus-preserving pancreatoduodenectomy: a comparative study of pancreatogastrostomy and pancreatojejunostomy. *Hepatogastroenterology*. 1999;46:1181–1186.
10. Jang JY, Kim SW, Park SJ, et al. Comparison of the functional outcome after pylorus-preserving pancreatoduodenectomy: pancreatogastrostomy and pancreatojejunostomy. *World J Surg*. 2002;26:366–371.
11. Ishikawa O, Ohigashi H, Eguchi H, et al. Long-term follow-up of glucose tolerance function after pancreaticoduodenectomy: comparison between pancreaticogastrostomy and pancreaticojejunostomy. *Surgery*. 2004;136:617–623.
12. Fang WL, Su CH, Shyr YM, et al. Functional and morphological changes in pancreatic remnant after pancreaticoduodenectomy. *Pancreas*. 2007;35:361–365.
13. Sato N, Yamaguchi K, Yokohata K, et al. Long-term morphological changes of remnant pancreas and biliary tree after pancreatoduodenectomy on CT. *Int Surg*. 1998;83:136–140.
14. Lemaire E, O'Toole D, Sauvanet A, et al. Functional and morphological changes in the pancreatic remnant following pancreaticoduodenectomy with pancreaticogastric anastomosis. *Br J Surg*. 2000;87:434–438.
15. Karasawa E, Goldberg HI, Moss AA, et al. CT pancreatogram in carcinoma of the pancreas and chronic pancreatitis. *Radiology*. 1983;148:489–493.
16. Telford GL, Ormsbee HS 3rd, Mason GR. Pancreaticogastrostomy improved by a pancreatic duct-to-gastric mucosa anastomosis. *Curr Surg*. 1980;37:140–142.
17. Amano H, Takada T, Ammori BJ, et al. Pancreatic duct patency after pancreaticogastrostomy: long-term follow-up study. *Hepatogastroenterology*. 1998;45:2382–2387.

11896 *Inorg. Chem.* **2009**, *48*, 11896–11902
DOI: 10.1021/ic902033c

Inorganic Chemistry
Article

New Strategy for Synthesis of Mercaptoundecahydrododecaborate Derivatives via Click Chemistry: Possible Boron Carriers and Visualization in Cells for Neutron Capture Therapy

Mohamed E. El-Zaria[†] and Hiroyuki Nakamura*

Department of Chemistry, Faculty of Science, Gakushuin University, 1-5-1 Mejiro, Toshima-ku, Tokyo 171-8588, Japan. [†]Permanent address: Department of Chemistry, Faculty of Science, University of Tanta, 31527-Tanta, Egypt.

Received October 14, 2009

A new method that utilizes the click cycloaddition reaction to functionalize $B_{12}H_{11}SH^{2-}$ (BSH) with organic molecules was investigated. *S,S*-Dipropargyl-$SB_{12}H_{11}^{-}$ (**1**) and *S*-propargyl-$SB_{12}H_{11}^{2-}$ (**4**) were prepared from $[(CH_3)_4N]_2B_{12}H_{11}SH$ and $[(CH_3)_4N]_2B_{12}H_{11}S(CH_2)_2CN$ (**2**) with propargyl bromide, respectively. Compound **1** or **4** reacted with various azides with mediation by Cu(II) ascorbate to give the corresponding bis-triazolo BSH derivatives (1-) or monotriazole BSH derivatives (2-), respectively, in excellent yields. The click cycloaddition reaction is very useful not only for the synthesis of various BSH-containing organic compounds for boron neutron capture therapy (BNCT) but also for the visualization of boron clusters in cells. We succeeded in the click cycloaddition reaction of compound **1** with Alexa Fluor 488 azide dye and found that **1** accumulated not in the cytoplasm but in the nuclei of HeLa cells.

Introduction

Boron neutron capture therapy (BNCT) is a special type of radiotherapy for cancer treatment by using ^{10}B compounds. A nuclear reaction occurs when ^{10}B is irradiated with thermal neutrons. This reaction yields an unstable intermediate, ^{11}B, which immediately undergoes fission to generate ^{7}Li and ^{4}He bearing approximately 2.4 MeV.[1,2] The particles dissipate their kinetic energies before traveling a distance equivalent to one cell diameter (~10 μm), enabling them to precisely kill tumor cells. Successful BNCT highly depends on the sufficient and selective boron delivery to the tumor cells. Therefore, the development of boron compounds that accumulate in the tumor cells in the appropriate concentrations is essential for BNCT. Various strategies have been studied to this end, including synthetic chemical approaches as well as biochemical and biophysical approaches.[3,4]

The disodium salt of mercaptoundecahydro-*closo*-dodecaborate ($Na_2B_{12}H_{11}SH$) has high boron content, an ionic nature, and significantly low toxicity based on its boron content. It was prepared for the first time more than 50 years ago.[5] The first clinical use of $Na_2B_{12}H_{11}SH$ was accomplished by Hatanaka in the 1960s for BNCT of patients with high-grade gliomas.[6,7] The potentially reactive sulfhydryl group in the $B_{12}H_{11}SH^{2-}$ (BSH) cluster is very important not only for transport into the brain tumor but also for functionalization with organic molecules.[8] Thus, numerous BSH-containing derivatives of biomolecules (e.g., porphyrins,[9–11] nitroimidazoles,[12] sugars,[13] and lipids[14–17]) have been synthesized

* To whom correspondence should be addressed. E-mail: hiroyuki.nakamura@gakushuin.ac.jp. Fax: +81-3-5992-1029.

(1) Soloway, A. H.; Tjarks, W.; Barnum, B. A.; Rong, F. G.; Barth, R. F.; Codogni, I. M.; Wilson, J. G. *Chem. Rev.* **1998**, *98*, 1515–1562.
(2) Yinghuai, Z.; Yan, K. C.; Maguire, J. A.; Hosmane, N. S. *Curr. Chem. Biol.* **2007**, *1*, 141–149.
(3) Barth, R. F.; Coderre, J. A.; Vicente, M. G.; Blue, T. E. *Clin. Cancer Res.* **2005**, *11*, 3987–4002.
(4) Barth, R. F. *Appl. Radiat. Isot.* **2009**, *67*, S3–S6.
(5) Soloway, A. H.; Hatanaka, H.; Davis, M. A. *J. Med. Chem.* **1967**, *10*, 714–717.
(6) Hatanaka, H. *J. Neurol.* **1975**, *209*, 81–94.
(7) Hatanaka, H.; Nakagawa, Y. *Int. J. Radiat. Oncol. Biol. Phys.* **1994**, *28*, 1061–1066.
(8) Gabel, D.; Moller, D.; Harfst, S.; Roesler, J.; Ketz, H. *Inorg. Chem.* **1993**, *32*, 2276–2278.
(9) Koo, M.-S.; Ozawa, T.; Santos, R. A.; Lamborn, K. R.; Bollen, A. W.; Deen, D. F.; Kahl, S. B. *J. Med. Chem.* **2007**, *50*, 820–827.
(10) Ratajski, M.; Osterloh, J.; Gabel, D. *Anti-Cancer Agents Med. Chem.* **2006**, *6*, 159–166.
(11) El-Zaria, M. E.; Ban, H.-S.; Nakamura, H. *Eur. J. Chem.* **2009**, in press.
(12) Masunaga, S.; Nagasawa, H.; Hiraoka, M.; Sakurai, Y.; Uto, Y.; Hori, H.; Nagata, K.; Suzuki, M.; Maruhashi, A.; Kinashi, Y.; Ono, K. *Appl. Radiat. Isot.* **2004**, *61*, 953–958.
(13) Lechtenberg, B.; Gabel, D. *J. Organomet. Chem.* **2005**, *690*, 2780–2782.
(14) Lee, J.-D.; Ueno, M.; Miyajima, Y.; Nakamura, H. *Org. Lett.* **2007**, *9*, 323–326.
(15) Nakamura, H.; Ueno, M.; Lee, J.-D.; Ban, H. S.; Justus, E.; Fan, P.; Gabel, D. *Tetrahedron Lett.* **2007**, *48*, 3151–3154.
(16) Justus, E.; Awad, D.; Hohnholt, M.; Schaffran, T.; Edwards, K.; Karlsson, G.; Damian, L.; Gabel, D. *Bioconjugate Chem.* **2007**, *18*, 1287–1293.
(17) Nakamura, H.; Lee, J.-D.; Ueno, M.; Miyajima, Y.; Ban, H. *NanoBiotechnology* **2007**, *3*, 135–145.

pubs.acs.org/IC

Published on Web 11/20/2009

for the development of tumor-targeting compounds. However, few strategies are available for the functionalization with organic molecules.

"Click chemistry" is a general term for a class of chemical transformations having a number of attractive features, including excellent functional group tolerance, high yield, and good selectivity under experimental conditions.[18,19] This is coupled with the use of readily available reagents and the avoidance of conventional chromatographic purification of the products. The Cu-catalyzed azide−alkyne cycloaddition reaction is one of the most reliable click reactions.[20,21] This reaction has enabled the practical and efficient preparation of 1,4-disubstituted-1,2,3-triazoles from an unprecedented range of substrates with excellent selectivity, which cannot be obtained with conventional Huisgen thermal approaches.[22] This has led to its application in a number of processes, including the synthesis of therapeutics,[23,24] protein-based biohybrids,[25,26] sugar arrays,[27] dendrimers,[28] and functional polymers.[29] The proposed mechanism for the Cu(I)-catalyzed reaction involves the addition of a Cu(I) acetylide to an azide in a stepwise sequence, giving a five-membered vinyl cuprate that yields the triazole products.[20,30] Recently, the facile synthesis of boronated chlorins,[31] hyaluronans,[32] and nucleotides[33,34] with click cycloaddition reactions was reported. In this paper, we report a simple and convenient procedure for the synthesis of BSH-containing organic molecules, based on the click cycloaddition reaction of organic azides with mono- and dipropargylic BSH derivatives. The current protocol enables us to synthesize a variety of BSH-containing biologically active compounds for BNCT.

Experimental Section

General Remarks. ^{1}H NMR and ^{13}C NMR spectra were measured on a JEOL JNM-AL 300 (300 MHz) and VARIAN UNITY-INOVA 400 (400 MHz) spectrometers. Chemical shifts of ^{1}H NMR and ^{13}C NMR were expressed in parts per million (ppm, δ units), and coupling constant (J) values were expressed in units of hertz (Hz). ^{11}B NMR spectra were recorded on a JEOL JNM-AL 300 spectrometer (96.3 MHz), and the chemical shifts were reported in δ units relative to external $BF_3 \cdot Et_2O$ in $CDCl_3$. IR (cm^{-1}) spectra were determined as KBr disk on a Shimadzu FTIR-8600PC spectrometer. Electron spray ionization (ESI) mass spectra were recorded on a Shimadzu LCMS-2010 eV spectrometer or Bruker Daltonics micro TOF-15 focus. Elemental analyses were performed by a CE instrument EA1110 CHNS-O automatic elemental analyzer. All compounds gave elemental analysis within ±0.4% of the theoretical values. Analytical thin layer chromatography (TLC) was performed on a glass plates of silica gel 60 GF_{254} (Merck). Visualization was accompanied by UV light (254 nm), I_2, $KMnO_4$, or $PdCl_2$. Preparative TLC was carried out using 0.75 mm layers of silica gel 60 GF_{254} (Merck) made from water slurries on glass plates of dimensions 20 × 20 cm^2, followed by drying in air at 100 °C. Column chromatography was conducted on silica gel (Merck Kieselgel 70−230 mesh). Most chemicals were of analytical grade and used without further purification. Azides (C_6H_5-CH_2N_3, *p*-Br-$C_6H_4CH_2N_3$, *p*-Me-$C_6H_4CH_2N_3$, *m*-CN-C_6H_4-CH_2N_3, *m*-MeO-$C_6H_4CH_2N_3$, $C_6H_5CH_2CH_2N_3$, and 3-azidopropyl-*o*-carborane), $[(CH_3)_4N]_2B_{12}H_{11}S(CH_2)_2CN$ **2**, and 1,2-*O*-distearoyl-*sn*-3-glycerol were prepared as described in literatures.[8,14,35,36]

***S,S*-Bis-(prop-2-ynyl)sulfonioundecahydro-*closo*-dodecaborate (1-) tetramethylammonium salt (1).** Bis-tetramethylammonium salt of BSH (1 g, 3.1 mmol) was dissolved in a mixture of acetonitrile/water (250 mL, 4:1) in a one-neck flask equipped with a dropping funnel. A solution of 3-bromo-1-propyne (1.3 mL, 17 mmol) in acetonitrile/water (40 mL, 4:1) was added dropwise at room temperature over a period of 10 min to the reaction mixture. After 24 h, the solvent was evaporated under vacuum, and the obtained solid was washed with ether and dissolved in acetonitrile. The inorganic salts were removed by filtration, and ether was added to the filtrate to precipitate the product **1** (840 mg, 84%) as the pale yellow solid. Crystallization from water is also possible for further purification, if necessary. mp over 300 °C. ^{1}H NMR (300 MHz, CD_3CN): δ 3.89 (m, 4H, S-CH_2), 3.07 (s, 12H, $N(CH_3)_4$), 2.81 (m, 2H, C≡CH), 1.8−0.55 (m, 11H, $B_{12}H_{11}$). ^{13}C NMR (75 MHz, CD_3CN): δ 77.87 (2C, C≡CH), 74.54 (2C, C≡CH), 56.23 (4C, $N(CH_3)_4$), 30.43 (2C, S-CH_2). ^{11}B NMR (96.3 MHz; CD_3CN): δ −15.59 (bs, 1B, B1), −18.98 (d, J_{BH} = 163.9 Hz, 11B, B2−12). IR (KBr, cm^{-1}): ν(CH) 3263 (m), 3030 (m), 2960 (S), ν(BH) 2495 (S), ν(C≡C) 2123 (w), ν(CH) 1485 (S), 1404 (W), 1286 (W), ν(B−B) 1045 (S), ν(CH) 995 (m), 948 (S), 821 (m), 719 (m), 673 (W). MS (ESI, negative): m/z 251.2 (M^-). Elemental analysis calcd for $C_{10}H_{29}B_{12}NS$: C, 36.94; H, 8.99; N, 4.31%. Found: C, 36.65; H, 8.89; N, 4.25%.

***S*-(Prop-2-ynyl)thioundecahydro-*closo*-dodecaborate (2-) bis-tetramethylammonium salt (4).** To a solution of **3** (340 mg, 1.0 mmol) in acetone (20 mL) was added 1 equiv of a 25% solution of $(CH_3)_4NOH$ in methanol dropwise. The white precipitate of the product formed immediately. The precipitate was filtered off and dried to give **4** (350 mg, 97%) as a white solid. mp 250−251 °C. ^{1}H NMR (300 MHz; DMSO): δ 3.58 (m, 2H, S-CH_2), 3.08 (s, 12H, $N(CH_3)_4$), 2.80 (m, 1H, C≡CH), 1.85−0.55 (m, 11H, $B_{12}H_{11}$). ^{13}C NMR (75 MHz; DMSO): δ 77.87 (1C, C≡CH), 72.54 (1C, C≡CH), 56.34 (8C, $N(CH_3)_4$), 36.87 (1C, S-CH_2). ^{11}B NMR (96.3 MHz; CD_3CN): δ −9.87 (bs, 1B, B1), −19.98 (d, J_{BH} = 161.7 Hz, 11B, B2−11), −21.59 (bs, 1B, B12). IR

(18) Kolb, H. C.; Finn, M. G.; Sharpless, K. B. *Angew. Chem., Int. Ed.* **2001**, *40*, 2004–2021.
(19) Kolb, H. C.; Sharpless, K. B. *Drug Discovery Today* **2003**, *8*, 1128–1137.
(20) Rostovtsev, V. V.; Green, L. G.; Fokin, V. V.; Sharpless, K. B. *Angew. Chem., Int. Ed.* **2002**, *41*, 2596–2599.
(21) Prescher, J. A.; Bertozzi, C. R. *Nat. Chem. Biol.* **2005**, *1*, 13–21.
(22) Huisgen, R. In *1,3-Dipolar Cycloaddition Chemistry*; Padwa, A., Ed.; Wiley: New York, 1984; Vol. *1*, pp 1−176.
(23) Lee, L. V.; Mitchell, M. L.; Huang, S.-J.; Fokin, V. V.; Sharpless, K. B.; Wong, C.-H. *J. Am. Chem. Soc.* **2003**, *125*, 9588–9589.
(24) Manetsch, R.; Krasinski, A.; Radic, Z.; Raushel, J.; Taylor, P.; Sharpless, K. B.; Kolb, H. C. *J. Am. Chem. Soc.* **2004**, *126*, 12809–12818.
(25) Speers, A. E.; Adam, G. C.; Cravatt, B. F. *J. Am. Chem. Soc.* **2003**, *125*, 4686–4687.
(26) Speers, A. E.; Cravatt, B. F. *Chem. Biol.* **2004**, *11*, 535–546.
(27) Fazio, F.; Bryan, M. C.; Blixt, O.; Paulson, J. C.; Wong, C.-H. *J. Am. Chem. Soc.* **2002**, *124*, 14397–14402.
(28) Wu, P.; Feldman, A. K.; Nugent, A. K.; Hawker, C. J.; Scheel, A.; Voit, B.; Pyun, J.; Fréchet, J. M. J.; Sharpless, K. B.; Fokin, V. V. *Angew. Chem., Int. Ed.* **2004**, *43*, 3928–3932.
(29) Mynar, J. L.; Hawker, C. J.; Frechet, J. M. J. *J. Am. Chem. Soc.* **2004**, *126*, 15020–15021.
(30) Himo, F.; Lovell, T.; Hilgraf, R.; Rostovtsev, V. V.; Noodleman, L.; Sharpless, K. B.; Fokin, V. V. *J. Am. Chem. Soc.* **2004**, *127*, 210–216.
(31) Bregadze, V. I.; Semioshkin, A. A.; Las'kova, J. N.; Berzina, M. Y.; Lobanova, I. A.; Sivaev, I. B.; Grin, M. A.; Titeev, R. A.; Brittal, D. I.; Ulyhina, O. V.; Chestnova, A. V.; Ignatova, A. A.; Feofanov, A. V.; Mironov, A. F. *Appl. Organomet. Chem.* **2009**, *23*, 370–374.
(32) Di Meo, C.; Luigi, P.; Campo, F.; Capitani, D.; Mannina, L.; Banzato, A.; Rondina, M.; Rosato, A.; Crescenzi, V. *Macromol. Biosci.* **2008**, *8*, 670–681.
(33) Olejniczak, A. B.; Wojtczak, B. A.; Lesnikowski, Z. J. *Nucl. Nucleic Acids* **2007**, *26*, 1611–1613.
(34) Wojtczak, B. A.; Andrysiak, A.; Grüner, B.; Lesnikowski, Z. J. *Chem.—Eur. J.* **2008**, *14*, 10675–10682.
(35) Benati, L.; Bencivenni, G.; Leardini, R.; Minozzi, M.; Nanni, D.; Scialpi, R.; Spagnolo, P.; Zanardi, G. *J. Org. Chem.* **2006**, *71*, 5822–5825.
(36) Wilson, J. G.; Anisuzzaman, A. K. M.; Alam, F.; Soloway, A. H. *Inorg. Chem.* **1992**, *31*, 1955–1958.

(KBr, cm^{-1}): ν(CH) 3265 (m), 3020 (m), 2965 (S). ν(BH) 2495 (S), ν(C≡C) 2125 (w), ν(CH) 1485 (S), 1405 (W), 1286 (W), ν(B−B) 1045 (S), ν(CH) 995 (m), 948 (S), 821 (m), 719 (m), 673 (W). ESI-MS: m/z 106.1 (106.1, M^{2-}). Elemental Analysis calcd for $C_{11}H_{38}B_{12}N_2S$: C, 36.68; H, 10.63; N, 7.78%. Found: C, 36.62; H, 10.49; N, 7.69%.

***S,S*-Bis[1-benzyl-(1,2,3-triazol-4-yl)methyl]sulfonioundecahydro-*closo*-dodecaborate (1-) tetramethylammonium salt (5).** To a solution of **1** (325 mg, 1 mmol) in acetonitrile (20 mL) were added $Cu(OAc)_2$ (50 mg, 0.27 mmol) and sodium ascorbate (100 mg, 0.5 mmol) at room temperature, and benzyl azide (333 mg, 2.5 mmol) was added dropwise with stirring. The reaction mixture was stirred for 2 h until complete consumption of **1** monitored by TLC ($MeOH/CH_2Cl_2$ 3:7). The mixture was filtered through a pad of Celite, and diethyl ether (10 mL) was added until a precipitate (inorganic salts) formed. This precipitate was removed by filtration, and another 200 mL of diethyl ether was added to the filtrate, whereupon a crystalline solid was precipitated. The finely crystalline product was filtered to give **5** (582 mg, 98%) as a white solid. For analysis a sample recrystallized again from acetonitrile/ether was obtained as colorless needles. mp 154−155 °C. ^{1}H NMR (300 MHz, CD_3CN): δ 7.79 (s, 2H, CH-triazole), 7.34 (m, 10H, CH-phenyl), 5.45 (s, 4H, CH_2-benzyl), 4.39 (m, 4H, S-CH_2), 3.07 (s, 12H, $N(CH_3)_4$), 1.87−0.65 (m, 11H, $B_{12}H_{11}$). ^{13}C NMR (75 MHz, CD_3CN): δ 136.36 (2C, C-triazole), 129.8, 129.27, 128.87 (12C, CH and C-phenyl), 125.97 (2C, CH-triazole), 56.2 (4C, (4C, $N(CH_3)_4$), 54.4 (2C, CH_2-benzyl), 37.35 (2C, S-CH_2). ^{11}B NMR (96.3 MHz; CD_3CN): δ −14.88 (bs, 1B, B1), −20.17 (d, J_{BH} = 151 Hz, 11B, B2−12). IR (KBr, cm^{-1}): ν(CH) 3406 (m), 3020 (W), 2918 (W). ν(BH) 2497 (S), ν(C=C) 1627 (m), ν(N=N) 1560 (W), ν(CH) 1485 (S), 1415 (W), 1286 (W), ν(B−B) 1045 (S), ν(CH) 995 (m), 941 (S), 835 (m), 742 (m), 685 (W). ESI-MS: m/z 517.5 (517.5, M^-). Elemental Analysis calcd for $C_{24}H_{43}B_{12}N_7S$: C, 48.74; H, 7.33; N, 16.58%. Found: C, 48.72; H, 7.28; N, 16.52%.

***S*-[1-Benzyl-1,2,3-triazol-4-yl)methyl]thioundecahydro-*closo*-dodecaborate (2-) bis-tetramethylammonium salt (12).** This compound was also prepared from **11** (473 mg, 1.0 mmol) using the procedure described for **4** to give a white solid of **11** (469 mg, 95%). Alternative procedure for synthesis of **12** is described as follows: To a solution of **4** (360 mg, 1 mmol) in acetonitrile-water (4:1, 20 mL) were added $Cu(OAc)_2$ (50 mg, 0.27 mmol) and sodium ascorbate (100 mg, 0.5 mmol) at room temperature, and benzyl azide (160 mg, 1.2 mmol) was added dropwise with stirring. The reaction mixture was stirred for 2 h until complete consumption of **4** monitored by TLC ($MeOH/CH_2Cl_2$ 3:7). The mixture was filtered off, and the solvent was removed under vacuum. The residue was purified by preparative TLC with $MeOH/CH_2Cl_2$ (3:7) as eluent to give **12** (369 mg, 77%) as a white solid. mp 235−236 °C. ^{1}H NMR (300 MHz; CD_3CN): δ 7.68 (s, 1H, CH-triazole), 7.34 (m, 5H, phenyl), 5.45 (s, 2H, CH_2-benzyl), 3.59 (m, 2H, S-CH_2), 3.16 (s, 24H, $N(CH_3)_4$), 0.39−1.71 (m, 11H, $B_{12}H_{11}$). ^{13}C NMR (75 MHz; CD_3CN): δ 137.52 (1C, CH-triazole), 129.65, 129.51, 129.15 (6C, CH and C-phenyl), 125.29 (1C, C-triazole), 54.47 (8C, $N(CH_3)_4$), 52.26 (1C, CH_2-benzyl), 37.52 (2C, S-CH_2). ^{11}B NMR (96.3 MHz; CD_3CN): δ −10.75 (bs, 1B, B1), −20.17 (d, J_{BH} = 86.7 Hz, 10B, B2−11), −22.58 (bs, 1B, B12) ppm. IR (KBr, cm^{-1}): ν(CH) 3388 (m), 3020 (m), 2935 (W). ν(BH) 2470 (S). ν(C=C) 1622 (m), ν(N=N) 1572 (W), ν(CH) 1487 (S), 1417 (W), 1288 (W), ν(B−B) 1049 (S), ν(CH) 992 (m), 948 (S), 837 (m), 745 (m), 689 (W). MS (ESI, negative): m/z 172.6 (172.6, M^-/2). Elemental analysis calcd for $C_{17}H_{37}B_{12}N_6S$: C, 43.82; H, 9.19; N, 14.19%. Found: C, 43.72; H, 9.17; N, 14.11%.

***S*-[1-(Benzyl-1,2,3-triazol-4-yl)methyl]-*S*-[1-(*m*-methoxybenzyl-1,2,3-triazol-4-yl)methyl]sulfonioundecahydro-*closo*-dodecaborate (1-) tetramethylammonium salt (14).** This compound was prepared from **13** (488 mg, 1 mmol) and benzyl azide (200 mg, 1.5 mmol), using the procedure described for **5** to give **14** (602 mg, 97%) as a white solid. mp 149−150 °C. ^{1}H NMR (300 MHz; CD_3CN): δ 8.09, 7.89 (s, 2H, CH-triazole), 7.27, 6.85 (m, 9H, CH-phenyl), 5.47 (m, 4H, CH_2-benzyl), 4.35 (m, 4H, S-CH_2), 3.7 (s, 3H, O−CH_3), 3.11 (s, 12H, $N(CH_3)_4$), 1.87−0.56 (m, 11H, $B_{12}H_{11}$). ^{13}C NMR (75 MHz; DMSO): δ 158.89 (2C, O-Cphenyl), 137.18, 136.84 (2C, C-triazole), 130.12, 129.97, 129.76, 125.35, 120.57, 119.89, 113.77, 113.45 (9C, CH and C-phenyl), 125.44 (2C, CH-triazole), 55.12 (1C, O−CH_3), 54.45 (4C, (4C, $N(CH_3)_4$), 52.72 (2C, CH_2-phenyl), 37.09, 36.67 (2C, S-CH_2). ^{11}B NMR (96.3 MHz; CD_3CN): δ −12.45 (bs, 1B, B1), −20.65 (d, J_{BH} = 151 Hz, 11B, B2−12). IR (KBr, cm^{-1}): ν(CH) 3445 (m), 3030 (W), 2928 (W), ν(BH) 2499 (S), ν(C=C) 1605 (m), ν(N=N) 1587 (W), ν(CH) 1485 (S), 1413 (W), 1286 (W), ν(B−B) 1047 (S), ν(CH) 995 (m), 948 (S), 821 (m), 758 (m), 721 (W). MS (ESI, negative): m/z 547.3 (M^-). Elemental analysis calcd for $C_{25}H_{45}B_{12}N_7OS$: C, 48.32; H, 7.3; N, 15.78%. Found: C, 48.09; H, 7.22; N, 15.56%.

***S,S*-Bis[1-(3-*o*-carboranylpropyl)-(1,2,3-triazol-4-yl)methyl]-sulfonioundecahydro-*closo*-dodecaborate (1-) tetramethylammonium salt (15).** This compound was prepared from **1** (325 mg, 1 mmol) and 3-azidopropyl-*o*-carborane (533 mg, 2.5 mmol), using the procedure described for **5** to give **15** (763 mg, 98%) as a white solid. mp 179−180 °C. ^{1}H NMR (300 MHz: CD_3CN): δ 7.9 (s, 2H, CH-triazole), 4.3 (m, 4H, N−CH_2-), 4.3 (m, 4H, S-CH_2), 4.3 (m, 2H, CH-carborane), 3.08 (s, 12H, $N(CH_3)_4$), 2.25 (m, 4H, −CH_2−), 2.03 (m, 4H, CH_2-carborane), 1.85−0.58 (m, 22H, $B_{22}H_{22}$). ^{13}C NMR (75 MHz; CD_3CN): δ 146.21 (2C, CH-triazole), 126.21 (2C, C-triazole), 76.16 (2C, C-carborane), 63.87 (2CH, CH-carborane) 56.15 (4C, (4C, $N(CH_3)_4$), 49.68 (2C, CH_2−N), 36.97 (2C, S-CH_2), 34.74 (2C, −CH_2−), 30.39 (2C, CH_2-carborane). ^{11}B NMR (96.3 MHz: CD_3CN): δ −7.89, −10.9 (bs, 2B, B1), −14.52, −16.5, −19.41, −20.04, −20.49 (bs, 20B, B2−12). IR (KBr, cm^{-1}): ν(CH) 3440 (m), 3043 (W), 2956 (W), ν(BH) 2584, 2492 (S), ν(C=C) 1620 (m), ν(N=N) 1575 (W), ν(CH) 1483 (S), 1413 (W), 1286 (W), ν(B−B) 1045 (S), ν(CH) 995 (m), 948 (S), 820 (m), 723 (m). MS (ESI, negative): m/z 705.7 (M^-). Elemental analysis calcd for $C_{20}H_{63}B_{32}N_7S$: C, 30.81; H, 8.14; N, 12.57%. Found: C, 30.74; H, 8.03; N, 12.52%.

***S,S*-Bis[1-(1,2-*O*-distearoyl-*sn*-3-glycerol)-(1′,2′,3′-triazole-4yl)-methyl]sulfonioundecahydro-*closo*-dodecaborate (1-) tetramethylammonium salt (18).** A mixture of **1** (163 mg, 0.5 mmol), $Cu(OAc)_2$ (50 mg, 0.27 mmol), and sodium ascorbate (100 mg, 0.5 mmol) in acetonitrile (20 mL) was stirred at 50 °C for 5 min. While stirring, **17** (815 mg, 1.25 mmol) was added dropwise. The reaction mixture was stirred at 50 °C for 2 h until complete consumption of **1** monitored by TLC ($MeOH/CH_2Cl_2$ 3:7). The mixture was filtered off and diethyl ether (10 mL) was added until a precipitate (inorganic salts) formed. This precipitate was removed by filtration, and another 100 mL of diethyl ether was added to the filtrate, whereupon a crystalline solid was precipitated. The finely crystalline product was collected by filtration to give a white solid of **18** (700 mg, 86%). For analysis a sample recrystallized again from acetonitrile/ether was obtained as almost colorless needles. mp 62−63 °C. ^{1}H NMR (300 MHz: $CDCl_3$): δ 7.66 (s, 2H, CH-triazole), 5.15 (m, 2H, CH−), 4.61 (m, 4H, N−CH_2−), 4.35 (m, 4H, S-CH_2), 4.33 (m, 4H, −$CHCH_2C$=O), 4.13 (m, 4H, $CHCH_2C$=O), 3.09 (s, 12H, $N(CH_3)_4$), 2.38 (m, 8H, −CH_2CH_2C=O), 1.85−0.55 (m, 11H, $B_{12}H_{11}$) 1.58 (m, 8H, CH_2), 1.22 (s, 80H, CH_2), 0.85 (t, 12H, J_{CH} = 12.61 Hz, CH_3). ^{13}C NMR (75 MHz: $CDCl_3$): δ 172.96, 172.83 (4C, CO), 136.85 (2C, CH-triazole), 127.0 (2C, C-triazole), 50.8 (4C, (4C, $N(CH_3)_4$), 38.69 (2C, S-CH_2), 69.83, 62.25, 34.15, 34.01, 31.89, 29.66, 29.59, 29.44, 29.33, 29.22, 29.07, 29.04, 28.88, 24.83, 24.78, 22.65, 14.07 (lipid-carbons). ^{11}B NMR (96.3 MHz; $CDCl_3$): δ −12.56 (bs, 1B, B1), −20.32 (bs, 11B, B2−12). IR (KBr, cm^{-1}): ν(CH) 2957 (m), 2920 (S), 2856 (S). ν(BH) 2499 (m), ν(C=O) 1741 (S), ν(C=C) 1625 (m). ν(N=N) 1572 (W), ν(CH) 1487 (m), 1467 (m), 1275 (W), ν(B−B) 1045 (S). ν(CH) 995 (m), 948 (S), 721 (m). ESI-MS: m/z 1551.5 (1551.5, M^-). Elemental analysis calcd for

Scheme 1

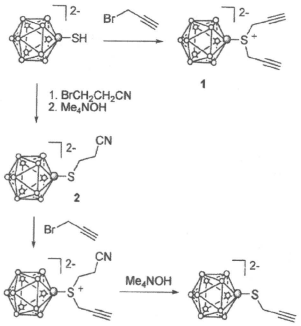

$C_{88}H_{179}B_{12}N_7O_8S$: C, 65.03; H, 11.1; N, 6.03%. Found: C, 64.91; H, 11.03; N, 5.89%.

Click Reaction in Cells. The human cervical carcinoma cell line HeLa cells were plated on p35 dishes (1×10^4 cells) containing 1 cm diameter glass coverslips and incubated at 37 °C for 24 h. After compound **1** treatment for 3 h, the cells were washed with PBS and fixed in 4% paraformaldehyde in PBS for 10 min. After washing with PBS, the cells were permeabilized with 0.1% Triton X-100 in PBS for 10 min, and blocked with 1% bovine serum albumin in PBS for 10 min. The click reactions with compound **1** and Alexa Fluor 488 azide (Alexa Fluor 488 5-carboxamide-(6-azidohexanyl), bis(triethylammonium salt), Invitrogen) were established with Click-iT Cell Reaction Buffer Kit (Invitrogen) according to the manufacturer's instructions. The cell nuclei were stained for 2 min with 100 nM DAPI. The cells were washed three times with PBS, mounted with Vectashield mounting medium (Vector), and analyzed under an Olympus IX71 fluorescence microscope.

Results and Discussion

Mono- and Dipropargylic BSH Derivatives. The synthesis of mono- and dipropargylic BSH derivatives is shown in Scheme 1. The bis-tetramethylammonium salt of BSH was treated with 5.5 equiv of 3-bromo-1-propyne in acetonitrile/water (4:1 v/v) to give *S*,*S*-dipropargyl-$SB_{12}H_{11}^-$ **1** in 87% yield. For the synthesis of monopropargylic BSH derivative **4**, we utilized Gabel's BSH protection protocol.[8] BSH was first converted into *S*,*S*-dicyanoethyl-$SB_{12}H_{11}^-$, which was treated with tetramethylammonium hydroxide for cleavage of one of two cyanoethyl groups to give protected BSH **2**. *S*-alkylation of **2** with 3-bromo-1-propyne proceeded in acetonitrile/water (4:1 v/v) to give *S*-cyanoethyl-*S*-propargyl-$SB_{12}H_{11}^-$ **3** in 65% yield. The deprotection of **3** by treatment with $(CH_3)_4NOH$ afforded *S*-propargyl-$SB_{12}H_{11}^-$ **4** in 95% yield.

Click Chemistry of Mono- and Dipropargylic BSH Derivatives. Click chemistry is an increasingly popular method for the rapid synthesis of novel biologically active compounds. By focusing research of new BNCT drugs on those that are available through these reliable and efficient reactions, click chemistry may accelerate the process of discovery and optimization. Three distinct features of click chemistry have called to our attention the possibility of applying this approach to the synthesis of BNCT agents: (1) the product is obtained in high yield without the need for further purification and without generating offensive byproducts; (2) the synthetic operation can be accomplished in a benign solvent, usually water; and (3) triazole units are heterocyclic structural motifs with considerable medicinal and agrochemical potential.[37]

Scheme 2

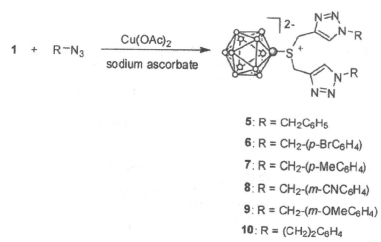

We first examined the click reaction of *S*,*S*-dipropargyl-$SB_{12}H_{11}^-$ **1** with 2.5 equiv of benzylazide at room temperature. By optimizing the reaction conditions, we found that $Cu(OAc)_2$ is a suitable source for the generation of Cu(I) species in situ in Huisgen's 1,3-dipolar cycloaddition reaction, as shown in Scheme 2. Sodium ascorbate proved to be an excellent reductant for this reaction.[38] Acetonitrile was found to be a suitable solvent because of the high solubility of both BSH-functionalized propynes and azides to give corresponding bis-triazoles **5** in 98% yield. As the reaction conditions were optimized, we employed them for further click reactions with various azides. The reactions proceeded smoothly in the presence of a semicatalytic amount of $Cu(OAc)_2$ and 0.5 equiv of sodium ascorbate at room temperature for 2 h, giving symmetric bis-triazolo BSH derivative (**5**–**10**) in 97–99% yields from **1**. Only the 1,4-disubstituted triazolo BSH derivatives were obtained (Scheme 2), in good agreement with the proposed reaction mechanism that the Cu(I) acetylide intermediate formed may undergo stepwise 1,3-dipolar cycloaddition with the azide, resulting in the regioselective product.[20,29]

We also examined the synthesis of monotriazole BSH derivative (**12**). Initial attempts to synthesize **12** by direct coupling of **4** with benzylazide in aqueous solution were unsuccessful because of the poor solubility of the azide. We found that the mixture of acetonitrile and water effectively promoted the reaction: the direct coupling of equimolar amounts of **4** and benzylazide proceeded in the presence of $Cu(OAc)_2$ and sodium ascorbate at room temperature in a mixture of acetonitrile and water (4:1 v/v) for 2 h. Compound **12** was isolated in 77% yield after purification by preparative TLC using CH_2Cl_2/MeOH (3:7 v/v) as eluent (Scheme 3). Another indirect route for the synthesis of **12** is the coupling reaction of **3** with benzylazide in acetonitrile under the same reaction conditions to

(37) Xia, Y.; Li, W.; Qu, F.; Fan, Z.; Liu, X.; Berro, C.; Rauzy, E.; Peng, L. *Org. Biomol. Chem.* **2007**, *5*, 1695–1701.
(38) Davis, M. B. *Polyhedron* **1992**, *11*, 285–321.

Scheme 3

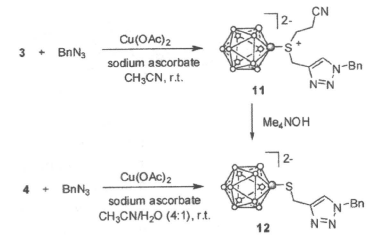

Scheme 4

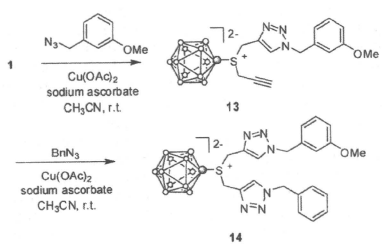

give **11** in 98% yield. Treatment of **11** with an equimolar amount of $(CH_3)_4NOH$ in acetone gave **12** in 95% yield (Scheme 3). Although the indirect method proceeds in two steps, compound **12** was isolated by reprecipitation from diethyl ether without the need for chromatographic workup.

The synthesis of an unsymmetric bis-triazolo BSH derivative (**13**) was also achieved by the stepwise click reactions of **1** with two different azides, as shown in Scheme 4. Treatment of **1** with an equimolar amount of *m*-methoxybenzylazide gave **13** in 88% yield. This provides an opportunity to intentionally preserve the unreacted propyne group for additional click reactions. Such compounds are important because the free propyne group can be used in click chemistry based fluorescence labeling methods for the visualization of boron compounds in cells incubated with azide-containing dyes. Similarly, the reaction of equimolar amounts of **13** with benzylazide gave BSH bearing two different triazole units (**14**) in 97% yield (Scheme 4). The reaction appears to be very safe and does not require any special precautions.

Candidates for Boron Carriers for BNCT. An efficient BNCT agent should be able to deliver a therapeutic amount of ^{10}B to tumors (> 20 μg/g) with high selectivity and low systemic toxicity.[1-4] The advantage of boron cluster containing compounds is that they can deliver high concentrations of boron to tumor cells with tolerable toxicity per molecule of BNCT agent administered. Polyhedral borane anions, such as *closo*-$B_{10}H_{10}^{2-}$ and *closo*-$B_{12}H_{12}^{2-}$, as well as carboranes, such as *closo*-$C_2B_{10}H_{12}$ and their corresponding *nido*-$C_2B_9H_{12}^-$, have been utilized for this purpose because of their known chemistry, hydrophilic/lipophilic property, high boron content, and chemical stability. Efforts to improve the efficacy of

Scheme 5

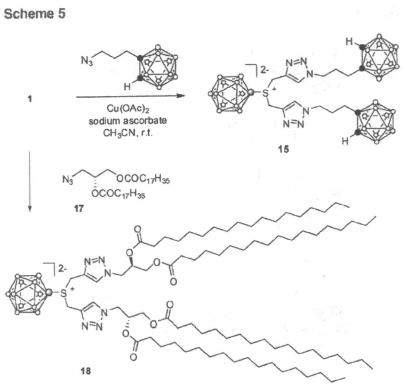

BNCT have focused on the development of novel boronated agents that have high boron content and exhibit selective uptake by tumor cells and favorable subcellular distribution.[39] Two drugs, $Na_2B_{12}H_{11}SH$ and *p*-boronophenylalanine (BPA), are used for the clinical treatment of glioblastoma and malignant melanoma patients, respectively, in BNCT.[40] Recently, the combination of BPA and BSH is utilized as BNCT's "cocktail" protocol for the treatment of glioblastoma and head and neck cancer patients.[41] Furthermore, the *tetrakis*-carborane carboxylate ester of 2,4-bis-(α,β-dihydroxyethyl)deuteroporphyrin-IX (BOPP)[42] was developed as an alternative candidate for boron carriers for BNCT. However, a phase I clinical study revealed its toxic side effects, most notably thrombocytopenia, which led to the limitation of its tolerable dose in humans.[43] The BNCT cocktail approach that utilizes a combination of BPA and BOPP has been demonstrated in mice bearing human undifferentiated thyroid cancer cells.[44]

Using the BNCT cocktail approach as reference, we synthesized high-boron-content compound **15** from **1** using the click cycloaddition reaction. Compound **1** was treated with 2.5 equiv of 3-azidopropyl-*o*-carborane[36] in the presence of $Cu(OAc)_2$ and sodium ascorbate in acetonitrile at room temperature to afford the bis-carborane-conjugated dodecaborate **15** in 98% yield (Scheme 5). The advantage of such compound bearing a high percentage of boron by weight (ca. 45%) is that it can potentially deliver high therapeutic amounts of boron to target

(39) Capala, J.; Barth, R. F.; Bailey, M. Q.; Fenstermaker, R. A.; Marek, M. J.; Rhodes, B. A. *Bioconjugate Chem.* **1997**, *8*, 289–295.
(40) Barth, R. F.; Yang, W.; Rotaru, J. H.; Moeschberger, M. L.; Boesel, C. P.; Soloway, A. H.; Joel, D. D.; Nawrocky, M. M.; Ono, K.; Goodman, J. H. *Radiat. Oncol. Biol. Phys.* **2000**, *47*, 209–218.
(41) Kato, I.; Ono, K.; Sakurai, Y.; Ohmae, M.; Maruhashi, A.; Imahori, Y.; Kirihata, M.; Nakazawa, M.; Yura, Y. *Appl. Radiat. Isot.* **2004**, *61*, 1069–1073.
(42) Kahl, S. B.; Koo, M.-S. *Chem. Commun.* **1990**, 1769–1771.
(43) Rosenthal, M. A.; Kavar, B.; Hill, J. S.; Morgan, D. J.; Nation, R. L.; Stylli, S. S.; Basser, R. L.; Uren, S.; Geldard, H.; Green, M. D.; Kahl, S. B.; Kaye, A. H. *J. Clin. Oncol.* **2001**, *19*, 519–524.
(44) Dagrosa, M. A.; Viaggi, M.; Rebagliati, R. J.; Batistoni, D.; Kahl, S. B.; Juvenal, G. J.; Pisarev, M. A. *Mol. Pharmaceutics* **2005**, *2*, 151–156.

tumor cells with tolerable toxicity. Moreover, it possesses the properties of two different boron cluster units (BSH and *o*-carborane). This new strategy in the synthesis of boronated compounds may be used to optimize BNCT with a cocktail of different boron clusters in one BNCT agent.

In addition to the BNCT cocktail approach, the liposomal boron delivery system has been attracting attention because it can deliver high therapeutic amounts of boron to tumor tissue.[45−49] Lipid carriers extravasate through the highly permeable microvessels of the tumors and remain locked in the interstitial fluid compartment because of the lack of functional lymphatic drainage.[50] Liposomes might therefore be useful vehicles for transporting boron to tumor tissue. Boron-containing lipids constitute very interesting building blocks for the construction of boron-containing liposomes and several approaches toward the synthesis of such lipids intended for incorporation into liposomes have been developed in our laboratory and others.[14−16,51−53]

In the present study, we demonstrated a new route for the preparation of a *closo*-dodecaborate lipid with a four-tailed moiety using click chemistry. For BSH coupling, it was necessary to prepare the requisite azide derivative of the lipid. The reaction of 1,2-*O*-distearoyl-*sn*-3-glycerol[14] with 1.2 equiv of *p*-tolylsulfonyl chloride gave **16** in 76% yield, which reacted with 5 equiv of sodium azide to obtain **17** in 90% yield after purification by column chromatography. The click cycloaddition reaction of **1** with azidolipid **17** was then performed in acetonitrile at 50 °C to give corresponding boronated lipid **18** in 86% yield (Scheme 5). In this case, a high temperature (50 °C) is necessary compared to the other cycloaddition reactions described in this paper because of the insolubility of azidolipid **17** in acetonitrile at room temperature.

Spectroscopic Studies. To gain information about the structures of the boronated compounds, NMR, IR, mass spectrometry, and elemental analysis were conducted. ^{1}H NMR signals for aliphatic hydrogens (C≡CH and CH_2) of **1** and **3** appeared at about 3.89 and 2.81 ppm, respectively, whereas ^{13}C NMR signals for CH, C, and CH_2 groups appeared at about 77.85, 74.5, and 30.5 ppm, respectively. These signals showed shifts to the high field region in both ^{1}H and ^{13}C NMR spectra of **4** upon removal of the cyanoethyl group in **3** by $(CH_3)_4NOH$. The ^{1}H and ^{13}C NMR spectra of the boronated compounds (**5**−**15** and **18**) revealed signals characteristic of both $B_{12}H_{11}S^{2-}$ derivatives and azide derivatives, with new signals corresponding to the triazole proton and the methylene group at N1 position of triazole. In the ^{1}H NMR spectrum of **13**, the signal at 2.85 ppm indicated the presence of a free alkyne group that is available for further coupling, as expected from the click cycloaddition reaction of **1** with *m*-methoxybenzyl azide in a 1:1 ratio. The structure of compound **16** was also confirmed by ^{1}H NMR spectroscopy, which showed new signals of the aromatic CH doublet at 7.92, 7.77, 7.4, and 7.34 ppm and a CH_3 singlet at 2.22 ppm. These signals disappeared in the ^{1}H NMR spectrum of azide **17**, and a new signal of the methylene group ($-CH_2N_3$) appeared at 3.43 ppm. The ^{11}B NMR spectra presented a characteristic shielding pattern over a quite remarkable range of about −19 to −15 ppm for **1**, **3**, **5**−**11**, **13**, **14**, and **18** and of about −9.5 to −22 ppm for **4** and **12**, showing only minor differences in the overall ^{11}B cluster shielding patterns. The ^{11}B NMR spectrum of **15** consisted of singlets at −7.8, −10.9, −14.5, and −16.5 ppm and multiplets in the range of −19.4 to −20.5 ppm with relative areas of 1:1:2:1:27. The high field singlets were assigned to three equatorial boron atoms, one apical boron atom of carboranes, and one apical boron atom of BSH cluster, respectively. The low field multiplets were assigned to 26 equatorial boron atoms of carboranes and the BSH cluster, as well as one apical boron atom of the BSH cluster.

Boronated compounds have characteristic stretching modes that are suitable for study by IR spectroscopy. The IR spectra of **1**, **3**, **4**, and **13** contained a weak absorption band located at about 2125 cm^{-1}, which could be attributed to the vibrational mode of the C≡C group. Free azide **17** exhibited a strong absorption band at 2160−2120 cm^{-1} because of the asymmetric stretching of the azide group, which occurred as a doublet. These were replaced with new medium and weak absorption bands within regions 1641−1602 and 1590−1555 cm^{-1}, which are characteristic of C=C and N=N groups, respectively. The ν(B−H) or the ν(B−B) were not sensitive to the click reactions. For compounds **1**, **3**, **4**−**15**, and **18**, ν(B−H) lay in the 2584−2499 cm^{-1} region, whereas ν(B−B) varied from 1049 to 1045 cm^{-1}. Among the frequencies of the $B_{12}H_{12}^{2-}$ moiety {ν(B−H) 2486 to 2462 cm^{-1}; ν(B−B) 1073 to 1057 cm^{-1}},[54] only slight differences were found among the compounds, indicating that intracluster bonding was not perturbed by the substitution of the icosahedron.

The negative-ion ESI mass spectra of compounds **1**, **3**, **5**−**11**, **13**−**15**, and **18** showed only the signal of a singly charged ion whose mass and typical isotopic pattern of boron isotopes (^{10}B and ^{11}B) suggest the molecular formula at $m/z = M^-$. The ESI mass spectra of **4** and **12** showed only the signal of the doubly charged molecular anion that was attributed to $m/z = M^-/2$.

Visualization of Compound 1 by Click Cycloaddition Reaction with Alexa Fluor 488 Azide in HeLa Cells. The development of technology for the chemical modification of compounds in, or on, living cells under physiological conditions has become an important issue for the dynamic imaging of drugs in medicinal chemistry. We examined the click cycloaddition reaction of compound **1** with Alexa Fluor 488 azide, which emits maximum

(45) Dreher, M. R.; Liu, W.; Michelich, C. R.; Dewhirst, M. W.; Yuan, F.; Chilkoti, A. *J. Natl. Cancer Inst.* **2006**, *98*, 335–344.
(46) Feakes, D. A.; Shelly, K.; Hawthorne, M. F. *Proc. Natl. Acad. Sci. U.S.A.* **1995**, *92*, 1367–1370.
(47) Watson-Clark, R. A.; Banquerigo, M. L.; Shelly, K.; Hawthorne, M. F.; Brahn, E. *Proc. Natl. Acad. Sci. U.S.A.* **1998**, *95*, 2531–2534.
(48) Yanagie, H.; Tomita, T.; Kobayashi, H.; Fujii, Y.; Takahashi, T.; Hasumi, K.; Nariuchi, H.; Sekiguchi, M. *Br. J. Cancer* **1991**, *63*, 522–526.
(49) Maruyama, K.; Ishida, O.; Kasaoka, S.; Takizawa, T.; Utoguchi, N.; Shinohara, A.; Chiba, M.; Kobayashi, H.; Eriguchi, M.; Yanagie, H. *J. Controlled Release* **2004**, *98*, 195–207.
(50) Pathak, A. P.; Artemov, D.; Ward, B. D.; Jackson, D. G.; Neeman, M.; Bhujwalla, Z. M. *Cancer Res.* **2005**, *65*, 1425–1432.
(51) Miyajima, Y.; Nakamura, H.; Kuwata, Y.; Lee, J.-D.; Masunaga, S.; Ono, K.; Maruyama, K. *Bioconjugate Chem.* **2006**, *17*, 1314–1320.
(52) Nakamura, H.; Miyajima, Y.; Takei, T.; Kasaoka, S.; Maruyama, K. *Chem. Commun.* **2004**, 1910–1911.
(53) Li, T.; Hamdi, J.; Hawthorne, M. F. *Bioconjugate Chem.* **2006**, *17*, 15–20.
(54) Srebny, H. G.; Preetz, W. *Z. Naturforsch.* **1984**, *39b*, 189–196.

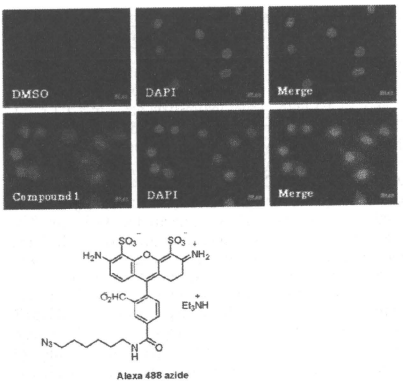

Figure 1. Click chemistry in cells. HeLa cells were incubated for 3 h with compound **1** (1 mM). After fixation and permeabilization of the cells, click reactions with compound **1** and Alexa Fluor 488 azide were performed, and the cell nuclei were stained with DAPI. The cells were analyzed under a fluorescence microscope.

fluorescence at 520 nm with excitation at 495 nm, in HeLa cells. The cells were plated on dishes containing 1 cm diameter glass coverslips and incubated at 37 °C for 24 h. Then, they were treated with compound **1** (1 mM) for 3 h. After fixing the cells with 4% paraformaldehyde in PBS for 10 min, the click cycloaddition reaction was performed with Alexa Fluor 488 azide. Cell nuclei were stained for 2 min with 100 nM 4′,6-diamino-2-phenylindole (DAPI). Fluorescence microscopy images are shown in Figure 1. HeLa cells treated with DMSO (without compound **1**) and Alexa Fluor 488 azide did not show any fluorescence except DAPI images (blue). In contrast, cells treated with compound **1** and Alexa Fluor 488 azide showed green fluorescence. The results indicate that compound **1** accumulating in the cells reacted with Alexa Fluor 488 azide in the cells and that the Alexa Fluor 488-conjugated *closo*-dodecaborates were illuminated by the fluorescence microscope. Interestingly, the fluorescence of the Alexa Fluor 488-conjugated *closo*-dodecaborates was observed mainly in the nuclei. Therefore, it was revealed that compound **1** accumulated not in the cytoplasm but in the nuclei of cells.

Conclusions

We have developed a new method to functionalize BSH with organic molecules. Our method focused on the synthesis of two classes of BSH terminal functionalized propyne groups: (*S*,*S*-dipropargyl-$SB_{12}H_{11}^-$: **1**) and (*S*-propargyl-$SB_{12}H_{11}^{2-}$: **4**). Compounds **1** and **4** acted as powerful building blocks for the synthesis of a broad spectrum of 1,4-disubstituted 1,2,3-triazole products in high yields based on the click cycloaddition reaction mediated by Cu(II) ascorbate. The current reactions require only benign reaction conditions and simple workup and purification procedures, and an unsymmetric bis-triazolo BSH derivative could also be synthesized by the stepwise click reaction. Compound **1** with 3-azidopropyl-*o*-carborane gave a high-boron-content compound having two different boron clusters (one BSH and two *o*-carboranes). The synthesis of BSH lipid with four-tailed moieties was also achieved by the click cycloaddition reaction of **1** with 3-*O*-azidoacetyl-1,2-*O*-distearoyl-*sn*-3-glycerol, which may be useful in the liposomal boron delivery system for neutron capture therapy. Finally, we demonstrated the click reaction of compound **1** with Alexa Fluor 488 azide in HeLa cells and found that compound **1** accumulated not in the cytoplasm but in the nuclei of the cells. We believe that this study not only provides synthetic applications but also clarifies the biological mechanism of BSH derivatives for neutron capture therapy.

Acknowledgment. We wish to acknowledge Dr. H.-S. Ban (Gakushuin Uinversity) for his contribution of biological experiments. This work was supported in part by Health and Labour Sciences Research Grants for Research on Nanotechnical Medical from the Ministry of Health, Labour and Welfare (20100201). M. E. El-Zaria thanks the Japan Society for the Promotion of Science (JSPS, ID No. P08363) for the financial support.

Note Added after ASAP Publication. This article was released ASAP on November 20, 2009. Reference 31 was updated and the correct version was posted on November 25, 2009.

Supporting Information Available: Detailed experimental procedures and characterization data of compounds **3**, **6**–**11**, **13**, **16**, and **17**. ^{11}B, ^{1}H, ^{13}C, and ^{13}C dept 135° NMR spectra of compounds (**1**–**18**). This material is available free of charge via the Internet at http://pubs.acs.org.

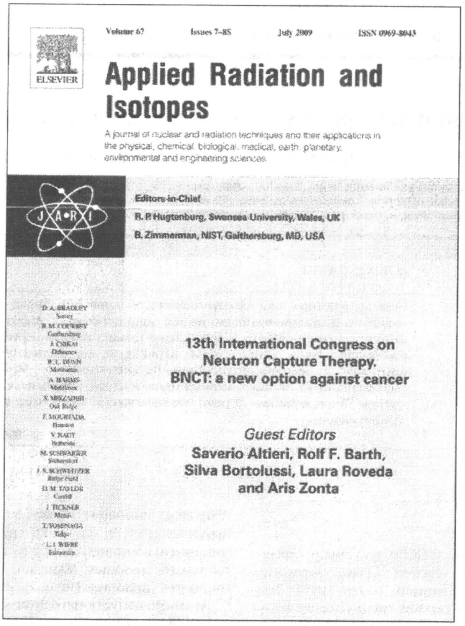

Applied Radiation and Isotopes 67 (2009) S84–S87

Contents lists available at ScienceDirect

Applied Radiation and Isotopes

journal homepage: www.elsevier.com/locate/apradiso

Development of boron nanocapsules for neutron capture therapy

H. Nakamura [a,*], M. Ueno [a], H.S. Ban [a], K. Nakai [b,c], K. Tsuruta [c], Y. Kaneda [b], A. Matsumura [c]

[a] Department of Chemistry, Faculty of Science, Gakushuin University, Mejiro, Tokyo 171-8588, Japan
[b] Division of Gene Therapy Science, Graduate School of Medicine, Osaka University, Osaka, 565-0871, Japan
[c] Department of Neurosurgery, Institute of Clinical Medicine, University of Tsukuba, Ibaragi, 305-8575, Japan

ARTICLE INFO

Keywords:
Closo-dodecaborate
Boron ion cluster lipids
Liposome
BSH

ABSTRACT

High accumulation and selective delivery of boron into tumor tissues are the most important requirements to achieve efficient neutron capture therapy of cancers. We focused on liposomal boron delivery system in order to achieve a large amount of boron delivery to tumor. We synthesized the double-tailed boron cluster lipid **4c** according to our reported procedure with modification. Size distribution of liposomes prepared from the boron cluster lipid **4c**, DMPC, PEG-DSPE, and cholesterol was determined as 100 nm in diameter by an electrophoretic light scattering spectrophotometer. A high level of ^{10}B concentration (22 ppm) was observed in tumor tissue at 24 h after the administration of boron liposomes.

1. Introduction

Boron neutron capture therapy (BNCT) is a binary cancer treatment based on the nuclear reaction of two essentially nontoxic species, ^{10}B and thermal neutrons (Locher, 1936). This therapy is based on the neutron capture reaction using non-radioactive ^{10}B, which produces an α-particle and a lithium-7 ion bearing approximately 2.4 MeV. These high linear energy transfer particles dissipate their kinetic energy before traveling one cell diameter (5–9 μM) in biological tissues, ensuring their potential precise cell killing. Therefore, high accumulation and selective delivery of boron into tumor tissue are the most important requirements to achieve efficient neutron capture therapy of cancers. There are three most important parameters for development of boron compounds: (1) achieving tumor concentrations in the range of 20–35 μg ^{10}B/g; (2) a tumor/normal tissue differential greater than 3–5; (3) sufficiently low toxicity (Barth et al., 2005). Recently, much attention has been paid for liposomal boron delivery system in order to accumulate a high concentration of boron into tumor. Yanagie first developed mercaptoundecahydrododecaborate (BSH)-encapsulated egg PC liposomes, which were conjugated with anti-human CEA (carcinoembryonic antigen) monoclonal antibody (Yanagie et al., 1991). Hawthorne prepared liposomes from distearoylphosphatidylcholine (DSPC) and cholesterol, in which various boron compounds were encapsulated (Shelly et al., 1992). Since their initial attempts, various boron clusters-encapsulated liposomes have been developed, such as PEGylated liposomes (Feakes et al., 1994), folate-conjugated liposomes (Pan et al., 2002), epidermal growth factor (EGF)-conjugated liposomes (Kullberg et al., 2003), transferrin (TF)-conjugated liposomes (Maruyama et al., 2004), and Cetuximab-conjugated liposomes (Pan et al., 2007).

As an alternative boron delivery system, a system involving the accumulation of boron in the liposomal bilayer is highly potent, because drugs can be encapsulated into the vacant inner cell of a liposome. Furthermore, functionalization of liposomes is possible by combination of lipid contents. Therefore, boron and drugs may be simultaneously delivered to tumor tissues for BNCT and chemotherapy of cancers. Hawthorne (Feakes et al., 1995) first introduced *nido*-carborane as a hydrophilic moiety into the amphiphile **1** (Fig. 1) and examined liposomal boron delivery in mice using **1** and distearoylphosphatidylcholine. We first developed the *nido*-carborane lipid **2**, which has a double-tailed moiety conjugated with *nido*-carborane as a hydrophilic function and demonstrated the vesicle formation (Nakamura et al., 2004). We investigated active targeting of the boronated liposomes to solid tumors by conjugation of transferrin to the surface of their liposomes. We observed a boron concentration of 22 μg ^{10}B/g tumor by the injection of the liposomes at 7.2 mg ^{10}B/kg body weight and longer survival rates of tumor bearing mice after BNCT (Miyajima et al., 2006). However, significant acute toxicity was observed in the mice injected at higher boron concentrations. Hawthorne and coworkers also recently reported synthesis of the *nido*-carborane lipid **3** and its unilamellar liposomes (Li et al., 2006). They pointed out the significant toxicity of the lipid **3** liposomes. In order to overcome this problem, we introduced BSH as an alternative hydrophilic function of boron lipids. BSH is significantly lowered toxicity and thus has been utilized for

* Corresponding author. Tel.: +81 339860221; fax: +81 359921029.
E-mail address: hiroyuki.nakamura@gakushuin.ac.jp (H. Nakamura).

0969-8043/$ - see front matter © 2009 Elsevier Ltd. All rights reserved.
doi:10.1016/j.apradiso.2009.03.091

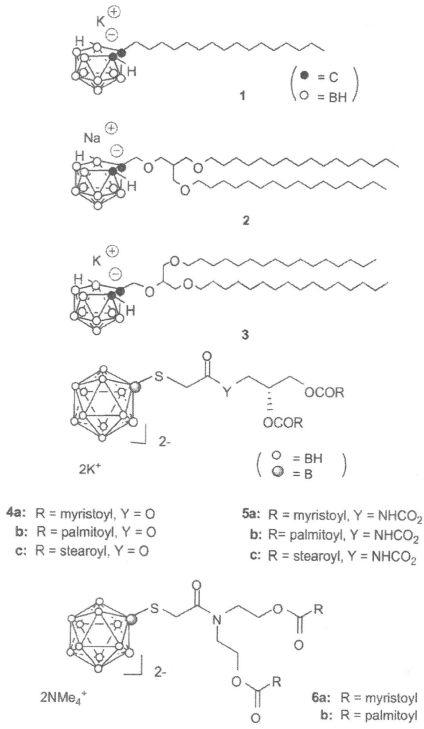

Fig. 1. Structures of boron cluster lipids.

clinical treatment of BNCT. Although few synthetic examples of BSH derivatives as boron carriers have been reported so far due to difficulty of their functionalizations, we have succeeded in the synthesis of *closo*-dodecaborate containing boron lipids **4a–c** and **5a–c** (Lee et al., 2007) using Gabel's novel *S*-alkylation of BSH protocol (Gabel et al., 1993). Symmetric *closo*-dodecaborate containing boron lipids **6** have been recently developed (Justus et al., 2007).

In this paper, we report the property and BNCT effects of liposomes prepared from *closo*-dodecaborate lipid **4c**.

2. Chemistry

Closo-dodecaborate containing boron lipid **4c** was prepared from (R)-(2,2-dimethyl-1,3-dioxolan-4-yl)methanol according to the procedure reported previously (Lee et al., 2007). The final deprotection step was modified by using potassium tertiary butoxide instead of tetramethylammonium hydroxide to afford the boron lipid **4c** as a potassium form (Fig. 2).

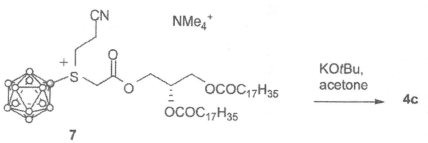

Fig. 2. Modified synthesis of the boron cluster lipid **4c** from **7**.

3. Preparation and size-distribution of liposomes

Liposomes with various boron content liposomes were prepared from cholesterol, distearoylphosphatidylcholine (DSPC), polyethyleneglycol-conjugated distearoylphosphatidylethanolamine (PEG-DSPE) and the boron cluster lipid **4c**, (1/1-X/0.1/X) by the reverse-phase evaporation (REV) method. The liposomes obtained were subjected to extrusion 10 times through a polycarbonate membrane of a 100 nm pore size, using an extruder at 60 °C. Purification was accomplished by ultracentrifuging at 200,000*g* for 60 min at 4 °C, and the pellets obtained were resuspended in PBS buffer. Liposome size was measured with an electrophoretic light scattering spectrophotometer. Fig. 3 shows the size distributions of the boron liposomes before- and after-extrusion. With increasing of the boron lipid content in liposomes, two major distribution peaks were observed before extrusion, although similar size distributions were obtained after extrusion.

4. Biodistribution and BNCT effects of liposomes

We next investigated the time-dependent biodistribution of the boronated liposomes prepared from **4c** in tumor-bearing mice (male BALB/c mice, seven weeks old), in which colon 26 cells were transplanted into their left thigh, via tail vein at a dose of 20 mg ^{10}B/kg (200 μL of a liposome solution). Enhanced accumulation of ^{10}B was observed in the liver and spleen and this does not conflict with the results of the biodistribution of the boron liposome prepared from **2** (Miyajima, 2006). A high level of ^{10}B concentration (22 ppm) was observed in tumor tissue at 24 h after the administration of boron liposomes. However, enhanced permeability and retention (EPR) effect was not observed and ^{10}B concentrations in tumor gradually decreased along with those in blood.

Besides the determination of ^{10}B concentration in various organs, the mice were anesthetized at 24 h after the administration of the boron liposomes and placed in an acrylic mouse holder, where their whole bodies, except their tumor-implanted leg, were shielded with acrylic resin. Neutron irradiation was carried out in JAEA atomic reactor (JRR-4). The tumor growth rate in mice given boron liposomes was significantly suppressed, although administration of saline did not reduce tumor growth after neutron irradiation. The detailed BNCT effects will be discussed elsewhere.

5. Conclusions

We synthesized the double-tailed boron cluster lipid **4c**, which have a $B_{12}H_{11}S$-moiety as a hydrophilic function. We investigated that similar size distributions were obtained after extrusion of liposomes prepared from cholesterol, DSPC, PEG-DSPE, and **4c** (1/1-X/0.1/X; X = 0.25~1). Furthermore, we found that no mouse died after injection with the boron liposomes at a dose of 20 mg ^{10}B/kg for up to three weeks. Since tumor growth rate in mice administrated with boron liposomes was significantly suppressed